

OBSERVATIONAL TESTS OF WORLD MODELS

Allan Sandage

Department of Physics and Astronomy, The Johns Hopkins University,
Baltimore, Maryland 21218 and Space Telescope Science Institute,
3700 San Martin Drive, Baltimore, Maryland 21218¹

1. THE ELEMENTS OF PRACTICAL COSMOLOGY

The standard model of cosmology, based on what has come to be called the Friedmann-Lemaître-Robertson-Walker (FLRW) model (hereinafter simply the Friedmann model), is now part of scientific culture. The most popular current version leads to the hot big bang (HBB) description of events near the beginning of the cosmic expansion, which has often been called a creation² moment at the beginning of physical time. In this review a prejudice in favor of the HBB [in contrast to cold beginnings discussed, for example, by Layzer (1987) in his remarkable book on the growth of order in the Universe] can hardly be suppressed, successful as the model has become in providing an understanding of the abundance of He⁴ and the 3-K radiation. Nevertheless, if a description of beginnings in this sense is to be confined within the methods of science rather than to be colored by teleological metaphysics, the model must pass the tests normal to science rather than to be accepted as revealed truth. The purpose of this

¹ Presently at Mount Wilson Observatory of the Carnegie Institution of Washington, 813 Santa Barbara Street, Pasadena, California 91101.

² *Creation* is a flammable word that triggers responses often not intended by writers who use it. Gamow, in reply to a critic who complained about the title of his famous book "The Creation of the Universe," advised his reader to interpret *creation* as something similar to a lady's fashion rather than to misinterpret it as a theological statement. If it were the latter, the inquiry would be removed from the possibility of using the scientific method to discover, rather than some other method to reveal. When *creation* is used in this review, its meaning is in the Gamow sense. Nevertheless, the subject is possibly as close as science can come to the questions of origins—hence its enormous appeal.

review is to discuss the direct tests of observation that lead to the view that a hot beginning to a current universe of finite age did occur.

Reviews of the theoretical aspects of the FLRW standard model from various viewpoints have appeared previously in this series. Novikov & Zeldovich (1967) surveyed the physical aspects of the HBB early Universe. Harrison (1973) summarized and discussed the various chemical eras, starting from a presumed initial singularity of very high temperature to the time of decoupling of matter and radiation, with the consequent formation of atoms some 30,000 yr after the Creation. Steigman (1976) reviewed the evidence and the reason(s) for the present matter-antimatter asymmetry. Boesgaard & Steigman (1985) discussed the theory and compared its predictions with observations of big bang nucleosynthesis. This comparison of the observed abundances of H, D, He³, He⁴, and Li⁷ with the calculations provides one of the two most powerful proofs of the HBB model. The other, of course, is the 3-K microwave background (MWB) radiation itself, discussed in these Reviews by Sunyaev & Zeldovich (1980) from the theoretical standpoint, and by Thaddeus (1972) and Weiss (1980) from the observational. The spectrum of the radiation resembles closely that of a blackbody. This is an important argument supporting a relic origin for the radiation, although alternate explanations have been proposed (Hoyle et al. 1968, Layzer & Hively 1973, Rana 1981, and references therein).

Other theoretical aspects of the standard model have been developed in these pages by Gould (1968) and Field (1972) in their reviews of the intergalactic medium, by Gott (1977) in his discussion of galaxy formation, and by Ellis (1984) in his survey of alternatives to the HBB standard model.

Particularly useful among the many workshop and conference proceedings that give entrance to the extensive archive literature are *Physical Cosmology* (Balian et al. 1979), *Astrophysical Cosmology* (Bruck et al. 1982), *Progress in Cosmology* (Wolfendale 1981), *Cosmology and Fundamental Physics* (Setti & Van Hove 1983), and *Inner Space/Outer Space* (Kolb et al. 1986).

Most of these discussions center on theoretical consequences of the HBB model. There have been only a few systematic reviews of results of the several direct (mostly geometrical) tests of the model. To be sure, important expositions of the principles of some of the classical tests are contained in discussions of the general properties of the models, such as the foundational reviews by Robertson (1933, 1955), the comprehensive summary by Zeldovich (1965), the lectures by Gunn (1978), and the textbooks by McVittie (1965), Peebles (1971), Weinberg (1972), Rowan-Robinson (1981), Narlikar (1983), and Zeldovich & Novikov (1983). But in all of

these accounts, details of the practical methods of the subject are kept as a black art, taken to be known, and therefore not set out in detail.

The present review is concerned with the observational aspects of the subject. This is because no textbook now exists on what every student should know if practical cosmology—the linchpin of the laboratory part of the subject—is to become their way of life. The emphasis is on the details of the calculations (i.e. the equations) that are necessary to make comparisons between the models and the data. My aim is to assess critically if the model does in fact have experimental verification beyond the admittedly very powerful tests of the Gamow, Alpher, and Herman 3-K radiation, and the consequent predictions of baryon and nucleosynthesis out of the HBB.

The most satisfactory outcome of any such test would be some direct verification of the curvature of space by an *experimental geometrical measurement* similar to those proposed by Gauss and by Karl Schwarzschild. Spatial curvature is *required* by the foundation of the theory, deeply buried as it is in the covering theory of general relativity (Section 2). Barring such a test (none has yet been successful), a direct verification that the redshift *is* due to a true expansion of the geometrical manifold would be most helpful, but again such a demonstration is not quite available yet (see Section 8).

One precise prediction of the theory is that the form of the redshift-distance relation [observed at fixed cosmic time—i.e. found by reducing the observed World *picture* to the World *map* (in the language of Milne) to account for the light travel time] be strictly linear, not exponential as in a “tired light” theory, nor in any other form as in some nonstandard models. Tests of the linearity of the redshift vector field are singularly robust and are featured later in this review.

One of the central requirements of the standard model is that the time since the Creation (defined here as the beginning of physical time) be related to the observed Hubble expansion rate H_0^{-1} by a factor that depends on the density parameter Ω_0 (in principle observable) via the connection (dictated by relativity) between the matter density and the space-time curvature. This relation is $kc^2/R^2 = H_0^2(\Omega_0 - 1)$ if the cosmological constant Λ is zero. Otherwise, the curvature has the additional term of $\Lambda c^2/3$ added. This test of the time scale, made by comparing the theoretical value of the age of the Universe, $T_0 = H_0^{-1}f(\Omega_0, \Lambda)$, with other clocks set ticking at the singularity, must work if the standard model is to be an adequate description. Because the test is so powerful, it has a chance to give a bona fide scientific judgment, if the relevant times can be accurately measured. We consider this test at length later in this review.

Finally, it is a commonplace that if any model is correct, it must have

verifiable predictive power. The HBB ideas would seem to have already passed the high hurdle of the 3-K MWB radiation first predicted by Gamow (1946, 1948) and his fellow "originalists" (Alpher 1948, Alpher et al. 1948, 1953, Alpher & Herman 1948, 1950) and later required by Peebles (1986), Wagoner et al. (1967), Wagoner (1973), and now so many others. The radiation was subsequently discovered by Penzias & Wilson (1965). At the time, Dicke et al. (1965) were engaged in a search whose purpose was in fact to verify their independent prediction as a requirement of a hot big bang.

The most elementary prediction of any model that does not postulate continuous creation is that the mean contents of the Universe (suitably spatially averaged) were once younger than they are now. Verification of this required evolution in the look-back time is yet nascent. The variety of observational tests using galaxies at different redshifts, i.e. at different look-back times, give suggestive but not yet quite overwhelming evidence for evolution with time (see Section 7).

In the sections that follow I assume no detailed familiarity with the theoretical literature, nor familiarity at all with the observations. We develop the necessary apparatus for the tests as we need them so as to lay bare the assumptions upon which they rest. The level is aimed at first-year graduate students to provide them entrance to the literature for the necessary data, equations, and correction tables.

The menu for this journey through the test maze begins with the simplest geometrical predictions of curved space. Here the galaxy number count-distance test is set out in its most direct form of the volume $V(r)$ enclosed within the "distance" l between us and coordinate point r in the comoving manifold (defined in the next section). Because the l distances are needed but are not themselves measured by rigid rods (suitably defined), we introduce next the distance-redshift relation that follows from the requirements of homogeneity and isotropy of the Robertson-Walker spaces. This leads naturally to the line element with its magic of accounting for the light-travel-time effects by using the null geodesic equation for light rays. This, in turn, permits direct entry to the redshift-distance equations, and therefrom to the redshift-luminosity (Mattig) relations for standard candles. This is the *Hubble diagram* straightaway. The practical details of corrections for aperture effect, K dimming, cluster richness, and the Bautz-Morgan contrast correlation are then set out. It is from the Hubble diagram for cluster galaxies that the linearity test for the form of the velocity field is most directly made.

Armed now with the $m(z, q_0)$ Mattig equation, the $N(z, q_0)$ count-redshift relation (as a function of space curvature) can be transformed to the observed $N(m, q_0)$ predictions, integrating over the luminosity function. It

is the comparison of this prediction with the observed $N(m)$ relation that motivated Hubble to claim a geometrical measurement of the space curvature (Section 5).

These developments dispose, then, of the $N(m, q_0)$ and the $m(z, q_0)$ tests, which are half of the four classical hopes (Sandage 1961a) to find the one World model.

The remaining two tests are the angular size–redshift relation, and the time-scale comparison. The angular size variation with redshift *should* be the most direct way to sample the geometry (Hoyle 1959). The theory of this test leads to the surface brightness $\sim (1+z)^{-4}$ relation, which must be valid if the expansion is real. Success in performing the experiment centers about the use of metric rather than isophotal galaxy diameters. The search for a suitable measure of a metric size is the present stumbling block, one yet to be adequately dislodged, but progress has been made (Section 8).

The time-scale test depends on the value of the Hubble expansion rate H_0 . The problems of its determination in the presence of observational bias in the data samples are set out in Section 9, where evidence favoring the long distance scale, which requires a low value of H_0 , is discussed.

2. EXPERIMENTAL GEOMETRY

2.1 *The Necessity for Space Curvature*

Is space curvature real? As an experimental problem, it becomes an epistemological question because of ambiguities in the definitions concerning the nature of the measuring rods and the character of the distances obtained with them (Section 2.2). As a theoretical problem, the *reality* of the formalism in the present physics (Einstein's theory of gravity) must be sought.

The non-Euclidean geometry, foreshadowed by Saccheri³ and invented by Gauss, Bolyai, and Lobachevski, was largely a curiosity for most scientists in the mid-nineteenth century, despite its central importance in this century, lying at the root of our present understanding of space-time. Unlike Saccheri, Gauss believed in its reality and proposed methods to

³The grip that our intuition holds on the mind concerning the unreality of non-Euclidean geometry prevented Saccheri from believing what his reason had discovered. E. T. Bell, in his book *Development of Mathematics*, writes, “[Saccheri’s] brilliant failure is one of the most remarkable instances in the history of mathematical thought of the mental inertia induced by an education in obedience and orthodoxy, confirmed in mature life by an excessive reverence for the perishable works of the immortal dead [Euclid]. With two geometries, each as valid as Euclid’s in his hand, Saccheri threw both away because he was willfully determined to continue in the obstinate worship of his idol, despite the insistent promptings of his own sane reason.”

measure the spatial curvature. K. Schwarzschild began such measurements by putting limits on the value of the curvature using the distribution of stellar parallaxes.

The intuitive geometry that is fixed on the senses by that outside spatial frame which gives us our ordinary experience seems Euclidean. Areas increase strictly as r^2 , volumes as r^3 , using the apparently common-sense definition of r . The concept of spatial curvature is foreign to the intuition and unreal to the nonscientist.

Nevertheless, if we take the structure of general relativity as *defining* reality, matter really does curve space. Particles move on straight lines in curved space instead of on curved paths in straight space. To be sure, we trade one mystery for another. The g_{ij} 's of the geometrical metric are determined by the distribution of matter, replacing Newton's force at a distance with geodesics in curved space. It is in this sense that general relativity has geometrized dynamics. The question remains, Is the curvature "real?" But what is reality? Indeed, has the question any verifiable meaning?

As an arguable definition, we could try "*for X to be real requires that X have effects.*"⁴ If we observe unmistakable effects we would say the thing "causing them" is real. It was the *absence* of predicted effects that removed the ether from reality. It was the verification of many predictions of its consequences that made the Lorentz transformation "real." Yet the Fitzgerald contraction as one "explanation" of the transformation is not real in this sense, but the time dilatation debatably is (Kennedy & Thorndike 1932), because *it* is observed, making the relativity of space-time equally real as long as no other explanation is possible.

On this definition space-time curvature is real. The predictions of its *effects* via Einstein's equations are well verified [see Will (1981) and Backer & Hellings (1986) for recent reviews]. The curvature is measured by the non-Euclidean g_{ij} 's. Yet areas and volumes are *not* measured. What actually is verified is that the formalism of the equations *works* in certain experimental circumstances (advance of Mercury's perihelion, time dilatation, a ray bending about the Sun, gravitational radiation, and perhaps even gravitational lensing).

However, the presence of space curvature would be more convincing if we had a simple direct proof that volumes fail to increase as r^3 , or that the

⁴This is similar to but not identical with a wider definition often used that "X is real if it is an essential element of a strongly confirmed theory." However, with both these definitions, a *reality* of this kind is ephemeral. If the theory is later found to be inadequate and must be replaced, the "reality" associated with it must also be replaced, and hence was not real in the ordinary usage of that word.

angular sizes of rods fail to decrease as r^{-1} in circumstances where the Riemann-Gauss scalar curvature, kc^2/R^2 , is expected to be nonzero. The full problem of defining relevant distances in the cosmology of ideal (congruent) spaces then becomes the central point in deciding the reality of space curvature.

2.2 *The Idea of Geometrical Experiments*

How then are we to measure deviations from Euclidean predictions? What rules concerning the properties of measuring rods do we adopt, and by what rules do we assess whether an experiment has given a non-Euclidean result? Early on, Poincaré denied the reality of actual curved space by stating that in any measurement that appeared to give a non-Euclidean result, one is at liberty to redefine the properties of the measuring rods in such a way as to recover a Euclidean prediction. A particularly interesting example of this, involving nonuniformly heated metal measuring rods, is given by Robertson (1949). Poincaré's point has been variously debated (cf. Whittaker 1958, Reichenbach 1958) with the consensus opinion being that contrived (unreasonable) explanations of changes in the measuring rods, if they are required to save the Euclidean case, are less desirable than a real Riemann-Lobachevski geometry. The debate then changes to the meaning of *contrived* and *unreasonable*. Consider again the Fitzgerald contraction of fast-moving measuring rods, and ultimately the reality of the Lorentz transformation. The issue is now resolved in Einstein's (1905) favor in that his deeper interpretation of space-time is viewed as more *reasonable* than the Fitzgerald explanation, which is now viewed as *contrived*.

In cosmology we are faced with similar problems. We cannot measure distances by placing rigid rods end to end. Rather, operational definitions of distance "by angular size," "by apparent luminosity," "by light travel time," or "by redshift" are perforce employed. Their use then requires a theory that connects the observables (luminosity, redshift, angular size) with the various notions of distances (McVittie 1974). One of the great initial surprises is that these distances differ from one another at large redshift, yet all have clear operational definitions. Which distance is "correct?" *All* are correct, of course, each consistent with their definition. Clearly, then, distance is a construct in the sense of Margenau (1950), operationally defined entirely by its method of measurement.

The best that astronomers can do is to connect the observables by a theory and test predictions of that theory when the equations are written in terms of the observables alone. To this end, the concept of distance becomes of heuristic value only. It is simply an auxiliary *parameter* that must drop from the final predictive equations.

But spatial curvature appears on a different footing. Although it too cannot be directly measured without a covering theory of “luminosity distance” or “redshift distance” to relate “volumes” to “distance,” the curvature does enter as a *primary* parameter (not to be dropped from the equations) in the predictive relations between the observables (luminosity, angular diameter, and redshift). The curvature is

$$\frac{kc^2}{R^2} = H_0^2(2q_0 - 1) \equiv H_0^2(\Omega_0 - 1) \quad 1.$$

if $\Lambda = 0$. The parameter q_0 (or Ω_0) enters into all the equations connecting redshift, luminosity, angular size, and number counts. In this sense, the curvature is measurable and therefore is “real,” because it has observable effects on the $m(z)$, $\theta(z)$, and $N(z)$ relations.

Direct experimental geometry is then a possibility, provided that we are willing to accept the equations that connect the q_0 measure of curvature with angles, areas, volumes, and redshifts—equations derived from some adopted cosmology.

2.3 Line Lengths and Areas on a Sphere of Constant Curvature

Experimental geometry can be illustrated by showing how the radius (of curvature) of a sphere can be found by measurements of line lengths, areas, and angles made entirely *on its surface*. The curvature $K = 1/R_1R_2$ is the product of the reciprocals of the radii of the two osculating circles to the geodesics drawn on the surface at any particular point P, put in the directions of maximum and minimum descent. Examples of surfaces of *constant* curvature are the sphere (where K is positive) and the pseudo-sphere (where K is negative).

Consider the experimental determination of the radius R (i.e. $K^{-1/2}$) of a sphere found by measuring lengths, areas, or angles on its surface. From any point P on the surface, proceed a distance r from P and draw a circle about P of radius r (*along the surface*). The length of this circle is

$$l = 2\pi R \sin(r/R), \quad 2.$$

which for r small compared with R is, to second order,

$$l = 2\pi r \left[1 - \frac{1}{6} \frac{r^2}{R^2} + O\left(\frac{r^4}{R^4}\right) \right]. \quad 3.$$

This differs from $2\pi r$ for a Euclidean plane ($K = 0$), permitting a determination of R once l and r are measured *on the surface itself!*

In a similar way, the areas of a spherical cap drawn about a point P with radius r along the surface is

$$A(r) = 2\pi R^2 \left(1 - \cos \frac{r}{R}\right). \quad 4.$$

For small r/R , Equation 4 can be expanded to

$$A(r) = \pi r^2 \left[1 - \frac{1}{12} \frac{r^2}{R^2} + O\left(\frac{r^4}{R^4}\right)\right], \quad 5.$$

which again differs from πr^2 for a space of zero curvature.

The deviation from Euclidean geometry is small. At the enormous distance of $r = R$, along the surface, Equation 4 shows that the area is $0.92\pi r^2$, differing from the Euclidean case by only 8%. This special case illustrates the general proposition that one must sample a very large fraction (i.e. of the order of curvature radius R) of any non-Euclidean space before deviations from the geometry of the Euclidean tangent space become measurable.

Besides lines and areas, the sum of the angles of triangles placed on the surface also measures the curvature. It can be shown that the difference of the angle sum from 180° for any triangle is the curvature times the area of the triangle, i.e.

$$\alpha + \beta + \delta - \pi = KA \quad 6.$$

where α , β , and δ are the interior angles of the triangle, and K is the curvature of the surface at the triangle. The special case of a hemisphere illustrates the theorem. The area of the hemisphere is $2\pi R^2$. The sum of the angles of the spherical triangle that forms the hemisphere is $2\pi + \pi/2 + \pi/2 = 3\pi$. The angular excess of $3\pi - \pi$ divided by the area is R^{-2} , which is the curvature K as stated by Equation 6. It can be shown that this equation holds for *any surface* of constant Gaussian curvature.

Note that Equations 2, 4, and 6, which measure different aspects of the geometry (lines, areas, and angles), all contain the common term $R^{-2} = K$. A case for the reality of space curvature would be strong if the measurements of quite a different nature that are required to test each of the three equations would give the same value of R^{-2} . In a similar way in cosmology, some confidence in the value of the geometrical parameter q_0 , which is related to the curvature via Equation 1, would obtain if multiple experiments of different kinds gave the same result. This congruence of answers is the goal of the observational quest.

Now to the details of the standard model.

2.4 The Volume $V(r)$ in Robertson-Walker Spaces

One supposes that the space that describes any real universe must be homogeneous and isotropic. Otherwise, the notion of extension as applied to material bodies would have a complicated meaning. By this is meant that any material body, transported to any region of the space, must be transformed into itself without tearing or buckling. Such spaces are congruent. They can be rotated into themselves by a coordinate transformation without shear. This is not true for nonhomogeneous, non-isotropic spaces.

Robertson (1929, 1935) and Walker (1936) verified that the most general expression for the geometrical interval dl^2 between two points in a space of constant curvature with coordinates r , θ , ϕ , and $r+dr$, $\theta+d\theta$, and $\phi+d\phi$ is

$$dl^2 = R^2(t) \left[\frac{dr^2}{1-kr^2} + r^2(d\theta^2 + \sin^2\theta d\phi^2) \right], \quad 7.$$

where k is the sign of the space curvature (+1 for $k > 0$, 0 for $k = 0$, -1 for $k < 0$). Various coordinate transformations give a variety of equivalent forms (e.g. McVittie 1956, 1965, Misner et al. 1973). Equation 7 is particularly convenient in deriving the various relations between the observable parameters and the geometry in the standard model.

The r , θ , ϕ numbers in Equation 7 are *comoving* coordinates. They are fixed (constant) for all time for a given galaxy. They are also *dimensionless*. The factor $R(t)$ is a scale factor (dimensions of length) that is a function of time in an expanding or contracting manifold. $R(t)$ is independent of r , θ , and ϕ in a congruent space (one of constant curvature).

The volume enclosed within the space from the origin ($r = 0$, put at the observer) and the coordinate value r is

$$V = 2\pi R^3 \int_0^r \frac{r^2 dr}{\sqrt{1-kr^2}} \int_0^{\pi/2} \sin\theta d\theta \int_0^{2\pi} d\phi. \quad 8.$$

For $k = 1$ this integrates to

$$V_1(r) = \frac{4\pi(Rr)^3}{3} \left[\frac{3}{2} \frac{\sin^{-1} r}{r^3} - \frac{3}{2} \frac{\sqrt{1-r^2}}{r^2} \right]; \quad 9.$$

for $k = -1$ to

$$V_{-1}(r) = \frac{4\pi(Rr)^3}{3} \left[\frac{3}{2} \frac{\sqrt{1+r^2}}{r^2} - \frac{3}{2} \frac{\sinh^{-1} r}{r^3} \right]; \quad 10.$$

and for $k = 0$ to

$$V_0(r) = \frac{4\pi R^3 r^3}{3}. \quad 11.$$

Note that r is not the *interval distance* from the origin to the point r, θ, ϕ . The manifold distance in the space described by Equation 7 is

$$l \equiv \int_{r=0}^r dl = R(t) \int_0^r \frac{dr}{\sqrt{1-kr^2}} = \begin{cases} R \sin^{-1} r & \text{for } k = +1, \\ Rr & \text{for } k = 0, \\ R \sinh^{-1} r & \text{for } k = -1, \end{cases} \quad 12.$$

without loss of generality by rotating the coordinate system into the $\theta = \phi = 0$ plane. Hence, the *coordinate* r in Equations 9–11 is given in terms of the ratio of the measured distance l to the scale factor R (i.e. l/R), just as in Equations 2 and 4. (There should be no confusion about the changed definitions of l and r between Equations 2, 4, and 8–12). Explicitly,

$$r = \begin{cases} \sin l/R & \text{for } k = +1, \\ l/R & \text{for } k = 0, \\ \sinh l/R & \text{for } k = -1. \end{cases} \quad 13.$$

Substituting Equation 13 into Equations 9, 10, and 11, and expanding for clarity to appreciate the dependence on the curvature, gives

$$V(l) = \frac{4\pi l^3}{3} \left[1 - \frac{k}{5} \frac{l^2}{R^2} + O\left(\frac{l^4}{R^4}\right) \right]. \quad 14.$$

By analogy with Equations 2 and 4, kR^{-2} is called the curvature of the space. Note that if $k = 0$, Equation 14 (i.e. Equation 11 also) gives the Euclidean volume.

The series expansion in Equation 14 illustrates the principle of the galaxy count-volume test. (In practice, of course, the exact equations are used.) If the distances l to a sample of galaxies were known and if a *complete* count of galaxies within this distance could be obtained, the curvature kR^{-2} could be measured by the excess (or deficiency) of the counts from an l^3 dependence. The distance l and hence the coordinate value of r (from Equation 13) are related to the redshift via the standard theory, to be developed in the next sections.

3. COUNT-REDSHIFT RELATION

3.1 The Coordinate r as a Function of Redshift

The relation between time and distance for a light ray is given by the null geodesic of the space-time interval whose metric is

$$ds^2 = c^2 dt^2 - R^2(t) \left[\frac{dr^2}{1-kr^2} + r^2(d\theta^2 + \sin^2\theta d\phi^2) \right]. \quad 15.$$

Orienting the axes so that $\theta = \phi = 0$ and putting $ds = 0$ gives the basic equation of the problem as

$$\int_0^r \frac{dr}{\sqrt{1-kr^2}} = c \int_{t_1}^{t_0} \frac{dt}{R(t)}. \quad 16.$$

Using Equation 12, we finally obtain

$$\begin{cases} \sin^{-1} r \\ r \\ \sinh^{-1} r \end{cases} = c \int_{t_1}^{t_0} \frac{dt}{R(t)} \quad (\text{for } k = +1, 0, -1), \quad 17.$$

which if $R(t)$ is a known function of time will give $r(t)$. This is related to the redshift $z \equiv \Delta\lambda/\lambda_0$ by the Lemaitre Equation

$$1 + z = \frac{R_0}{R_1}, \quad 18.$$

where R_0 and R_1 are the scale factors at the times of light reception and light emission, respectively.

The time variation of R is given by the solution of the dynamical Friedmann equation

$$\left(\frac{\dot{R}}{R}\right)^2 + \frac{2\ddot{R}}{R} = -\frac{kc^2}{R^2}, \quad 19.$$

which is fundamental to the standard model. Integration of this equation gives $R(t)$, which when put in Equation 17 gives the $r(z)$ connection via Equation 18. This in turn, when put in Equations 9–11 gives $V(z)$, which solves the problem in closed form.

Two special cases illustrate the method. Consider first the Euclidean case of $k = 0$. The well-known solution of Equation 19 for $R(t_i)$ at time t_i is

$$R(t_i) = R(t_0)(t_i/t_0)^{2/3}. \quad 20.$$

When this is put into the right side of Equation 17 and integrated, using Equation 18 to relate z with the ratio of the scale factors, we obtain

$$r = \frac{3ct_0}{R_0} \left[1 - \frac{1}{\sqrt{1+z}} \right], \quad 21.$$

which, with $t_0 = 2/3H_0^{-1}$, where $H_0 = \dot{R}/R$, gives

$$R_0 r = \frac{2c}{H_0} \left[1 - \frac{1}{\sqrt{1+z}} \right]. \quad 22.$$

This, put into Equation 11, gives

$$V(z) = \frac{32\pi c^3}{3H_0^3} \left[1 - \frac{1}{\sqrt{1+z}} \right]^3 \quad 23.$$

for the volume enclosed in redshift distance z for the Euclidean case ($k = 0$).

Consider next an empty universe (no mass). In this case, $\ddot{R} = 0$, $k = -1$, and Equation 19 integrates directly to

$$R(t_i) = R_0(t_0)(t_i/t_0). \quad 24.$$

Equation 24 put into the right side of Equation 17 gives

$$\sinh^{-1} r = \frac{ct_0}{R_0} \ln(1+z). \quad 25.$$

Noting that $t_0 = H_0^{-1}$ in this case, we obtain, after reduction,

$$R_0 r = \frac{c}{H_0} \left(\frac{z}{1+z} \right) \left(1 + \frac{z}{2} \right). \quad 26.$$

Using Equation 1, and remembering that $q_0 = -\ddot{R}_0/R_0H_0^2 = 0$ in this case, gives $R_0 = c/H_0$, hence

$$r = \left(\frac{z}{1+z} \right) \left(1 + \frac{z}{2} \right). \quad 27.$$

Equations 26 and 27, substituted into Equation 10, give $V(z)$ for an empty universe explicitly.

We have now introduced the dimensionless deceleration parameter q_0 , which is convenient in expressing the general case. This parameter first arose in the literature via series expansions of the relevant observational equations (Heckmann 1942, Robertson 1955, McVittie 1956, Davidson 1959), where no recourse to the solution of the Friedmann equation was needed. Before Mattig's (1958, 1959) exact (closed) solutions were known, Taylor expansions of $R(t)$ were made backward in time starting with the time of observation t_0 . This required no knowledge of the Friedmann solu-

tion but merely an assumption that $R(t)$ is well enough behaved for a Taylor series to exist. These series expressions for the $V(z)$, $m(z)$, and $\theta(z)$ tests sufficed for small redshifts, but not for redshifts of arbitrarily large size. In contrast, Equations 21, 22, 26, 27 are *exact* for all values of z . It follows that their use in Equations 9 and 10 for the volumes also apply to any value of the redshift. The reason is that we have used the complete solution for $R(t)$ from Equation 19 in Equation 17 rather than a Taylor series.

The value of q_0 determines the size of the space curvature via Equation 1. This, in turn, is related to the matter density (Hoyle & Sandage 1956) by

$$\rho = \frac{3H^2}{4\pi G} q_0. \quad 28.$$

For any arbitrary ρ value (hence q_0 value) we seek general formulae for $r(z)$ and $Rr(z)$. Equations 21, 22, 26, and 27 are special cases of these formulae. We need the general solution of the Friedmann equation (Equation 19) for any arbitrary value of the curvature kc^2/R^2 .

Mattig (1958) shows that this solution is

$$r = \frac{(2q_0 - 1)^{1/2}}{q_0^2(1+z)} [zq_0 + (q_0 - 1)\{-1 + (2q_0z + 1)^{1/2}\}] \quad 29.$$

and

$$R_0 r = \frac{c}{H_0 q_0^2(1+z)} [zq_0 + (q_0 - 1)\{-1 + (2q_0z + 1)^{1/2}\}] \quad 30.$$

for all values of q_0 . A transparent derivation of these equations in terms of the parametric cycloid and hypercycloid development angle was given by Sandage (1961b).

3.2 The Predicted $N(z, q_0)$ Relation

Combining Equations 9–11 with Equations 29 and 30 gives the exact $N(z, q_0)$ relation, calculated therefrom directly in parametric form. A calculation via this route shows the dependence of $N(z)$ on curvature for three q_0 values in Figure 1. The normalization of the volume is arbitrary in this diagram; $N(z)$ is proportional to $V(z)$, the proportionality factor being the volume density of galaxies.

The lowest value of q_0 shown in Figure 1 is that which is required by adding the luminosity density of galaxies obtained from the observed $N(m)$ data. As discussed by Binggeli et al. (1988) in their review of the luminosity function in this volume, this minimum permissible value of q_0 is

$$2q_0 = 1.5 \times 10^{-3}(M/L), \quad 31.$$

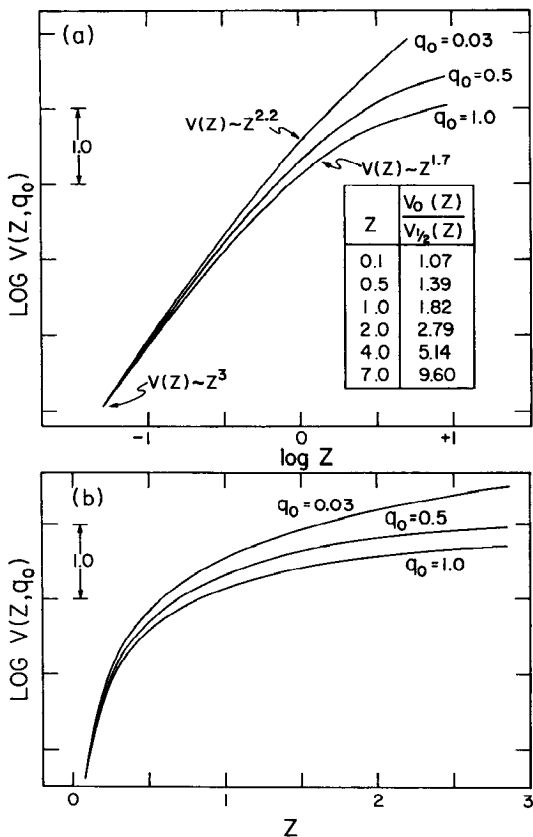


Figure 1 Theoretical $N(z, q_0)$ relations for three values of q_0 . Plotted is the integral count, i.e. the total number of galaxies in a complete (volume-limited) sample that have redshifts smaller than z . Parts (a) and (b) are the same function but plotted as $\log z$ (a) and z (b).

which is $q_0 = 0.03$ if $M/L = 40$. The second case shown in Figure 1 is for $\Omega_0 = 1$ ($q_0 = 1/2$) required by Grand Unification. The third case ($q_0 = 1$) is for a highly curved Riemannian space of curvature $c^2/R^2 = H_0^2$. If $H_0 = 50 \text{ km s}^{-1} \text{ Mpc}^{-1}$, the radius of curvature would be $R = 6000 \text{ Mpc}$, which is only 300 times the distance to the Virgo cluster!

Figure 1a shows $N(z, q_0)$ vs. $\log z$. Figure 1b is the same calculation, but it is displayed in z rather than $\log z$. The marked interval along the ordinate is a factor of 10 in the counts. For small redshifts ($z < 0.1$) the slope of $N(z)$ curves for all reasonable q_0 is $d \log N(z)/dz = 3$, becoming considerably flatter for higher redshifts, as marked along the curves in Figure

1a. For large redshifts, the volume becomes much smaller than the z^3 Euclidean case for $q_0 > 1/2$, but larger for the hyperbolic geometry of $q_0 < 0.5$. The ratio of the volumes encompassed from the observer to redshift z for $q_0 = 0$ compared with $q_0 = 0.5$ is shown as a function of z in the table in Figure 1a.

4. THE REDSHIFT-MAGNITUDE EQUATION

4.1 *The Predicted Hubble Diagram With No Luminosity Evolution*

The $N(z, q_0)$ volume-redshift relation of the last section is very difficult to apply in practice because complete galaxy counts in *redshift space* require redshift measurements of every galaxy (of all types and surface brightness) in the volume, or else a correction for sample incompleteness in a redshift survey that is complete to a given magnitude limit (Loh & Spillar 1986, Loh 1986). These corrections must be highly precise if the small differences in the $N(m, q_0)$ curves in Figure 1 are to be measured. For this reason, the value of q_0 via this route is quite uncertain at the moment.

The easier test observationally is the count-magnitude relation, $N(m, q_0)$, used in its most elementary form by Hubble (1936b), following the theory set out by Hubble & Tolman (1935) for $N(r)$. We now cast their discussion into modern form by using the closed equation for the apparent magnitude-redshift relation via the Mattig equations and thereby changing $N(z, q_0)$ into the $N(m, q_0)$ count-magnitude prediction.

The apparent bolometric flux f_b received at Earth from a galaxy receding with redshift z whose absolute flux (at the source) is F_b was shown by Robertson (1938) (after some debate) to be

$$f_b = \frac{F_b}{4\pi(R_0 r)^2(1+z)^2}. \quad 32.$$

For an appreciation of this equation, consider a sphere of interval radius l (Equations 12, 13) centered on the source, over which the flux of a light pulse is spread at the time of light reception, t_0 , at the Earth. The area of this sphere is not $4\pi l^2$ if the geometry is non-Euclidean but is, rather, $4\pi(R_0 r)^2$, where $R_0 r = R_0 \sin l/R$ using Equation 12 for $k = +1$. As in the case of the spherical cap of Equation 5, this area is smaller than $4\pi l^2$ owing to the spatial curvature if $k = +1$, or larger if $k = -1$:

$$A(l) = 4\pi l^2 \left[1 - \frac{1}{3} \frac{l^2 k}{R_0^2} + O\left(\frac{l^4}{R_0^4}\right) \right].$$

The difference in the area compared with the Euclidean case is accounted

for in Equation 32 by the $(R_0 r)^2$ factor rather than by simply using the interval distance l , which would be incorrect. The $(1+z)^2$ term accounts for the energy depletion and dilution factors of the radiation due to the redshift. One factor arises because each photon is decreased in energy by $(1+z)$, and hence the entire ensemble is depleted by the same factor. The second factor of $(1+z)$ is present if the redshift is due to true expansion. It is caused by the increased path length, with the consequent decrease in the energy *density*. If the Universe is *not* expanding, the second $(1+z)$ factor would not be present, a crucial point for the surface brightness test discussed in Section 8.

Converting Equation 32 into magnitudes and using Equation 30 for $(R_0 r)^2$ gives the theoretical $m(z, q_0)$ equation for the Hubble diagram in terms of the *bolometric* magnitude:

$$m_{\text{bol}} = M_{\text{bol}} + 5 \log q_0^{-2} [z q_0 + (q_0 - 1) \{-1 + (2q_0 z + 1)^{1/2}\}] + C, \quad 33.$$

where the constant C is $2.5 \log 4\pi + 5 \log c/H_0$. Note that the factor $(1+z)^2$ of Equation 32 is incorporated in Equation 33 as part of the theory. Some earlier writers, following Hubble, included the $-5 \log(1+z)$ factor as a correction term to the observed magnitudes (as part of a generalized K term). This is not the modern practice, however, which, as done here, carries this factor into Equation 33 via Equation 32. This point is very important if the reader is to understand Hubble's (1936b) method of correction, which differs fundamentally from the modern practice, based on the equations given here.

Series expansion of Equation 33 gives the well-known equation (e.g. Robertson 1955, McVittie 1956)

$$m_{\text{bol}} = 5 \log z + 1.086(1 - q_0)z + O(z^2) \quad 34.$$

used by Humason et al. (1956; hereinafter HMS) in their early analysis of cluster data. Although adequate to $z \sim 0.3$, the deviations of Equation 34 from Equation 33 for larger z become inadequately large (cf. Mattig 1958, his Figure 1).

4.2 Conversion of Observed Heterochromatic Apparent Magnitude to the Apparent Bolometric Scale:

The K Correction

The shift of the spectrum toward the red causes observed apparent magnitudes to differ from those that would have been observed at zero redshift. The correction is due to the fixed detector effective wavelength and the finite detector bandwidth. As defined in current usage (HMS, appendix B; Oke & Sandage 1968), it is composed of two terms. The *effective* bandwidth

in the rest frame of the source is *smaller* than in the rest frame of the observer because the source spectrum is stretched upon redshift. Each rest-frame wavelength λ_0 appears to the observer at $\lambda_0(1+z)$, whereas the detector bandwidth $\Delta\lambda_0$ is generally fixed. The bandwidth term due to this stretching is $2.5 \log(1+z)$ magnitudes, in the sense that the corrected magnitude must be brighter than the observed. The color-selective term is the ratio of the flux of the redshifted spectrum to the unshifted spectrum that is accepted by the detector. The term can be calculated by quadrature once the rest-frame spectral energy distribution (SED) of the source is known (the second term in Equation B7 of HMS).

Lack of accurate knowledge of the K correction was a stumbling block in the early interpretations of (a) the galaxy counts (Hubble 1936b, Greenstein 1938), (b) the $m(z)$ magnitude-redshift relation (Hubble 1953, HMS), and (c) the color evolution (Stebbins & Whitford 1948). Because of its crucial role in the interpretation of these cosmological test data, great effort was made from 1960 to 1975 to measure the SED of galaxies of various Hubble types. Early emphasis was put on E and S0 galaxies because of their dominance as first-ranked cluster galaxies. However, for the galaxy count problem in the field, $K(z)$ values for spirals of all Hubble classes (Sa, Sb, Sc, Sd, Sm, Im) are also required, together with knowledge of the fractional morphological mix of the sample.

Following Stebbins & Whitford's (1948) early six-color broadband measurements that gave highly smoothed $I(\lambda)$ distributions (see also Whitford 1954), Code (1959) and Oke & Sandage (1968) obtained spectrum scanner data at 50 and 25 Å resolution of bright E galaxies. A study using intermediate-band photometry was also made by Lasker (1970). These gave the first modern K corrections during the 1970s, although the data referred only to the central ~ 15 -arcsec regions of E galaxies in the Leo and Virgo clusters. Because the centers of E and S0 galaxies are redder than the outer regions (de Vaucouleurs 1960, Tift 1963, 1969, de Vaucouleurs & de Vaucouleurs 1972, Sandage & Visvanathan 1978), these nuclear $K(z)$ values were too large by progressive factors that reach ~ 0.1 mag at $z \sim 0.3$ (Whitford 1971, his Figure 2). Schild & Oke (1971) and Whitford (1971) then used very large aperture photometry to account for the color gradient. From their integrated SEDs they calculated $K(z)$ values in the B , V , and R photometric bands to redshifts of $z = 0.28$ for B and of $z = 0.60$ for V and R , but again only for E and S0 galaxies. Oke (1971) then obtained spectral scans of three *distant* (at that time) first-ranked cluster galaxies at redshifts of $z = 0.2$, $z = 0.38$, and $z = 0.46$, giving usable SEDs for E galaxies to $\lambda_0 = 2700$ Å in the rest frame. This permitted $K(B)$ to be calculated to $z = 0.52$ and $K(V)$ and $K(R)$ to $z = 0.72$ on the assumption of no color evolution.

Wells (1972) measured $I(\lambda)$ from 3500 to 5500 Å for a range of galaxy types. Using these data, to which OAO-2 data (Code et al. 1972) were added in the near-UV, Pence (1976) calculated K corrections for all galaxy types to large redshifts, giving very useful comprehensive tables. Further UV data were added by Ellis et al. (1977). Using the final reduced data from the OAO-2, Code & Welch (1979) calculated new K corrections to redshifts of $z = 1$. Using these data, together with new observations made with the ANS satellite, Coleman et al. (1980) calculated $I(\lambda)$ energy distributions for old stellar populations and for Sbc, Scd, and Im galaxies to $\lambda_0 = 1400$ Å and gave comprehensive K corrections in the U , B , V , and R photometric bands to $z = 2$. These data are the most extensive K corrections now available in the standard broadband photometric system, providing an enormous advance in this crucial problem since the early analysis by HMS. Sebok (1986), using the energy distributions of Wells, listed $K(z)$ for all morphological types for the Thuan-Gunn red system. Schneider et al. (1983a) list $K(z)$ for the Thuan-Gunn g , r , i , and z bands for giant E and S0 galaxies.

A summary of the SEDs in the archive literature that have been used to calculate K and the color variations with z is given by Yoshii & Takahara (1988) in their valuable review of cosmological tests.

4.3 *The Predicted Hubble Diagram With Correction for Luminosity Evolution*

In an evolving universe, the mean age of galaxies decreases with increasing redshift simply because we sample earlier times as we look out in distance. A first estimate of the expected change of E galaxy luminosities with look-back time, based on the change of the turnoff luminosity in the HR diagram for an old coeval population, gave a mean evolutionary rate of $L \sim t^{-4/3}$ for a flat luminosity function at the main sequence turnoff (Sandage 1961b). Because the luminosity function is not flat but rises for faint magnitudes below the turnoff, this is an *upper* limit, overestimating the luminosity rate by about 30%.

Call the change of magnitude due to evolution $E(t)$, Equation 33, transformed to heterochromatic magnitudes, then becomes

$$m_\lambda = M_\lambda - K_\lambda(z) - E_\lambda(t) + 5 \log q_0^{-2} \times [zq_0 + (q_0 - 1) \{-1 + (2q_0z + 1)^{1/2}\}] + C, \quad 35.$$

which is a basic equation that is used extensively in the following sections.

As for the size of $E(t)$, the simple evolution rate for an old coeval population of $L \sim t^{-4/3}$ quoted above would give a magnitude variation of $\Delta \text{mag} = -2.5 \log t_0/t_1$, where t_0 and t_1 are the ages of the source at light

reception at the Earth and at light emission from the source, respectively. If $t_0 = 15 \times 10^9$ yr and we inquire for the case of a look-back time of 10^9 yr, then $\Delta \text{mag} = -2.5 \log(15/14)^{4/3} = 0.10$ mag for small t_0/t . The sense of the correction is that galaxies were brighter in the past. If this rate is $\sim 30\%$ too high (Tinsley & Gunn 1976), the rough estimate of $E(t)$ is then ~ 0.07 mag per 10^9 yr.

Elaborate calculations of $E(t)$ form the subject of galaxy evolution via stellar population synthesis, pioneered by Tinsley (1968, 1972a,b, 1976, 1977a,b, 1980, and references therein) and her colleagues. The exact rate depends on the various assumptions of star formation rates over time and on the slope of the main sequence luminosity function. However, order-of-magnitude corrections, changing t to z via equations in the next section, give $\Delta m \approx -2.5 \log(1+z)$. For small z the correction again is approximately 0.07 mag per 10^9 yr on a time scale of $t_0 \sim 15 \times 10^9$ yr for the age of the Universe—nearly the same as the early, quite elementary estimates.

For *very* large redshifts, where the look-back times are of the order of the age of the Universe, much more elaborate evolutionary models are required than simple main sequence burn-down rates near the present main sequence termination point. The philosophy by which the rates can be calculated near the beginning of galaxy formation was first set out by Tinsley (1968). Modern calculations include those of Bruzual & Kron (1980), Bruzual (1981, 1983a,b), and Arimoto & Yoshii (1986, 1987). A summary of $E(t)$ over the age range of 10^7 to 1.5×10^{10} yr is given by Yoshii & Takahara (1988, their Figure 2) for E/S0 and Sdm galaxies in the *UBVRIJK* photometric bands.

4.4 The Look-Back Time as a Function of A and q_0

To use Equation 35 we must change $E(t)$ into $E(z)$ by the relation between the look-back time $\tau = t_0 - t_1$ and the redshift as a function of q_0 . The general case requires the closed solution of $R(t)$ from the Friedmann equation. Before setting down this general solution, it is instructive to consider again the simple cases of $q_0 = 0$ and $q_0 = 1/2$ for empty space and for flat space-time, respectively.

Recall that $R(t) \sim t$ for $q_0 = 0$ and $R(t) \sim t^{2/3}$ for $q_0 = 1/2$. Using these dependencies and the Lemaitre equation of $R_0/R_1 = 1+z$ gives the following relations for the look-back time:

$$\tau = H_0^{-1} \left(\frac{z}{1+z} \right) \quad \text{for } q_0 = 0, \quad 36.$$

$$\tau = \frac{2}{3} H_0^{-1} \left[1 - \frac{1}{(1+z)^{3/2}} \right] \quad \text{for } q_0 = 1/2. \quad 37.$$

The general case for any q_0 is found by combining the age equations (Sandage 1961a, Equations 61 and 65) of $T_0 = f(q_0, H_0)$ with the $R_0/R_1 = q(z, q_0)$ Friedmann solution, together with $R_0/R_1 = 1 + z$. Tables are given in Sandage (1961b).

5. PREDICTED AND OBSERVED COUNT-MAGNITUDE RELATION

5.1 *Method of Predicting $N(m, q_0, E)$ for an Infinitely Narrow Luminosity Function*

The necessary apparatus is now in place to predict the expected $N(m)$ relation for any assumed q_0 value and luminosity evolution rate $E(z)$. The $N(z)$ relation calculated by the method of Section 3.2 can be transformed to $N(m, q_0, E)$ using Equation 35. The conversion is trivial if M is assumed to be a fixed number, $\langle M \rangle$, with no dispersion (i.e. if the luminosity function is a spike). In this case, for computational purposes the equations are easiest used progressively in parametric form with the following steps, once q_0 has been fixed for a particular geometry.

1. For any particular redshift z , calculate r and rR_0 from Equations 29 and 30.
2. Use Equations 9, 10, or 11 (depending on the value of k) to calculate $V(z)$, which aside from a normalization factor is the $N(z, q_0)$ of Section 3.2.
3. For any z and q_0 use Equation 35 to calculate m for an assumed absolute magnitude $\langle M \rangle$, using the $K(z)$ and $E(z)$ corrections.
4. Repeat for a variety of z and q_0 values, producing the predicted family of $N(m, q_0)$ curves.

These steps are the method that was used to show numerically the degeneracy of $N(m)$ to q_0 to first order in z (Sandage 1961a, his Figures 4 and 5) if $E(z) = 0$, despite the nondegeneracy to q_0 in $N(z)$. The same result that $N(m)$ is less sensitive to q_0 than is $N(z)$ was shown analytically by Robertson & Noonan (1968), Misner et al. (1973), and Brown & Tinsley (1974) using series expansions. The reason for the near-degeneracy of the $N(m)$ counts to q_0 is that although the $N(z)$ relation is relatively sensitive to q_0 , its dependence on q_0 appears with the opposite sign from the variation of $m(z)$ with q_0 in Equation 35. This nearly cancels the curvature dependence of $N(m, q_0)$. The calculated $N(m, q_0)$ curves with no K correction (i.e. using the m_{bol} magnitude scale) are shown in Figure 2 for $q_0 = 0$ and $q_0 = 0.5$. For this idealized calculation, all galaxies were assumed to have the same absolute magnitude of $M_{\text{bol}} = -20.5$; this is a reasonable value,

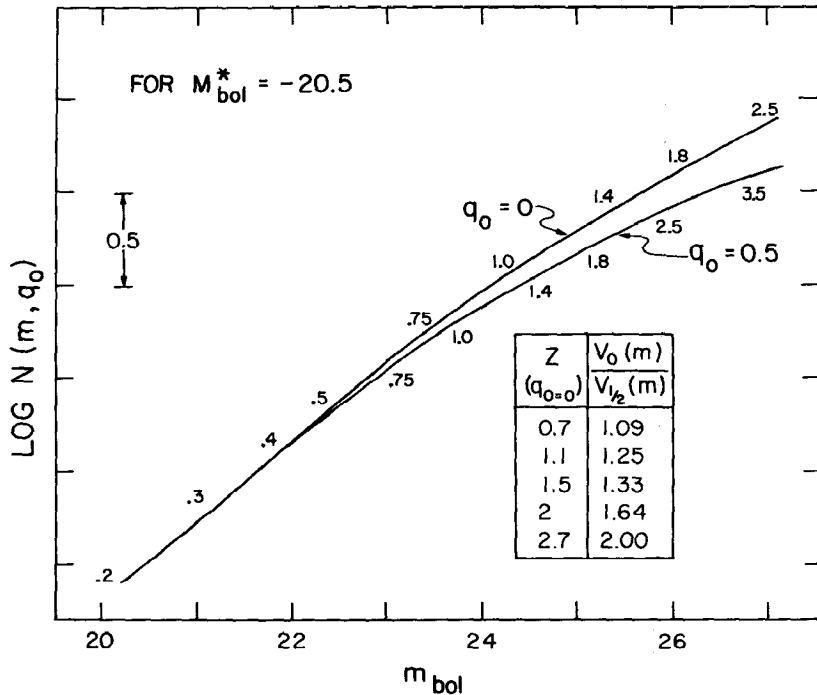


Figure 2 Theoretical $N(m, q_0)$ relations for two values of q_0 using bolometric magnitudes (i.e. no K correction has been applied) for galaxies with no spread in absolute luminosity. In practice, K corrections for each galaxy type must be applied for the particular detector band, and integrations must be performed over the luminosity functions for each morphological type and summed over the morphological mix, making the dependence on q_0 smaller than in this limiting example. Redshift values are shown along each curve.

close to M_{\downarrow}^* for the field luminosity function for high-surface-brightness galaxies (Tammann et al. 1979) in the *Revised Shapley-Ames Catalog* (Sandage & Tammann 1981; hereinafter RSA).

The redshift is marked along each curve in Figure 2, showing the different z values at a given m_{bol} value depending on q_0 given by Equation 35. The volume ratios at various z values (for $q_0 = 0$) are listed in the table interior to the diagram.

It is therefore surprising that Yee & Green (1987) claim a determination of q_0 from faint galaxy counts. They find a nonnegligible dependence on q_0 (their Figures 4 and 5). This result is probably produced by the strong dependence of the $E(z)$ evolutionary correction on q_0 (their Table 3), presumably due to the q_0 dependence in the conversion of $E(t)$ to $E(z)$, as explained above. The determination of q_0 in this way is then not a direct

test of different *volumes* of a non-Euclidean geometry (i.e. the direct volume test) but rather a much more indirect route that connects secular luminosity evolution with a *time scale* that does depend on H_0 and q_0 (Section 9).

5.2 *The Full Complication of the $N(m, q_0, E)$ Prediction, Given $E(z)$ and the Luminosity Function $\Phi(M, T)$*

For the real case we must integrate over the luminosity function. Because this function changes in shape and normalization with galaxy type (Binggeli 1987, Binggeli et al. 1988) and because $K(z)$ in Equation 35 is also a strong function of type, separate integrations are required for each Hubble morphological class. The results for a given type are then summed over all types using an assumed galaxy mix.

The integration over absolute luminosity, and over the sheets and voids of the galaxy distribution, is done by the usual equation of stellar statistics:

$$A(m, T) = C \int_0^z D(z, T) \phi(M, T) dV(z, q_0), \quad 38.$$

where $A(m, T)$ is the number of galaxies of type T per unit area at m in interval dm , C is a normalization factor used to convert the absolute density (in number of galaxies of type T per cubic parsec) to units of number of galaxies per unit area, $D(z, T)$ is the density at distance z of type T , $\phi(M, T)$ is the luminosity function read at M in interval dM for galaxies of type T , and $dV(z, q_0)$ is the volume element between redshift z_1 and z_2 corresponding to the magnitude interval between $m - dm$ and $m + dm$.

The total number of galaxies brighter than m is

$$N(m, q_0) = \int_T \int_0^m A(m, T) dT dm, \quad 39.$$

i.e. $A(m, T)$ summed over type and magnitude.

To apply Equation 38 we must use Equations 9–11, 29, and 30 for $V(z, q_0)$, together with the $m(M, z, q_0, E)$ relation of Equation 35. In this way, all variables in Equation 38 can be related to each other, albeit in a multiparametric way.

The simplest practical method for solving Equation 38 is to replace the integral by a summation over shells bounded by redshifts z_1 and z_2 , such that the apparent magnitude [for fixed $M - K(z) - E(z)$ values] at z_2 differs by one magnitude from that at z_1 . An $m, \log \pi$ -like table can then be constructed by the method of Kapteyn (cf. Bok 1931, 1937, Mihalas & Binney 1981). Such a table has cells separated by a unit apparent magnitude interval along the top of each column and by z_1 and z_2 boundaries

for the rows. In each $(m, z_1 - z_2)$ cell a particular $M - K(z) - E(z)$ value applies via Equation 35. The volume element in each row, given by Equations 9–11, 29, and 30, can be multiplied by the (M, T) and $D(z)$ that applies to each cell [i.e. at a given $\langle z \rangle = 1/2(z_1 + z_2)$]. The sum of each column is the $A(m)$ value for a given type. The process is then repeated for each type, and the $A(m)$ values are summed via Equation 38 to give $N(m, q_0)$.

This, or an equivalent method, has presumably been used by those who compare galaxy counts with predictions of the models, although the methods have not been described in detail in any of the original archive papers in the literature, now to be discussed.

5.3 Observations

5.3.1 RESULTS BEFORE ~1970 Galaxy counts were used near the beginning of this century to study the surface distribution of nebulae in efforts to establish their nature. Seares' (1925) definitive paper (a) established the latitude dependence, (b) emphasized the zone of avoidance, and (c) rediscovered the north Galactic pole anomaly [following Humboldt (1866) (quoted by Zwicky 1957)], a feature now called the Local Supercluster (de Vaucouleurs 1956). Seares' work, following that of Proctor (1869), Hinks (1911), Fath (1914), Hardcastle (1914), and Reynolds (1920, 1923a,b), struck at the heart of these surface distribution problems, solving them in principle and preceding Hubble's (1931, 1934) massive study with its straightforward definitive presentation.

Shortly after his discovery of Cepheids in M31 and NGC 6822 (Hubble 1925a,b), Hubble (1926) wrote his central paper on the general properties of galaxies. As part of the discussion, he analyzed galaxy number counts over the magnitude range $m_{pg} = 8.5-16.7$ from various earlier sources. These data provided the first reliable $N(m)$ relation, showing that $\log N(m) = 0.6m + \text{constant}$. The coefficient for m was 0.6 to within the error, showing beyond doubt (and for the first time) that nebulae are distributed homogeneously *in the large* (i.e. when averaged over an appreciable solid angle). The same conclusion was reached by Shapley & Ames (1932, their Figure 6) from counts brighter than $m_{pg} = 13$. The slope coefficient of $\log N(m)$ is 0.6 for any homogeneously distributed luminous sources, no matter what their luminosity distribution, provided only that the geometry is at least approximately Euclidean (von der Pahlen 1937, Bok 1937).

Hubble's demonstration that $\log N(m)$ varies as $0.6m$ was a crucial proof that galaxies provide a fair sample with which to study the large-scale matter distribution of the Universe. Galaxies are not merely a local phenomenon as part of a larger hierarchy. To be sure, larger structures of

clusters of galaxies and clusters of clusters do exist. Shapley (1932), Bok (1934), and Hubble (1934, his Figure 7) did discuss the clustering tendency. Nevertheless, grand averages at various distances, taken over large-enough solid angles, show no sign of progressive diminution from homogeneity (Sandage et al. 1972) as would be present in a Charlier-like hierarchy [but see de Vaucouleurs (1970) for an opposite opinion].

Galaxy counts to magnitudes fainter than 16.7 were made by Hubble (1934), Mayall (1934), and again by Hubble (1936b), giving five additional points for $N(m)$ at $m = 18.1, 18.8, 19.1, 20.0,$ and 21.0 on the magnitude scale extant in 1936.

Analyzing these data, Hubble (1936b, 1937) concluded that the *spatial curvature* had been robustly detected. But its radius of curvature was so small, if the magnitude correction terms due to redshift were correct, to cause him to question if the redshift was due to a true expansion. His analysis followed the formalism developed by Hubble & Tolman (1935), applying the $K(z)$ correction *and also the $(1+z)^2$ term of Equation 32 to the data*. Hubble stated that the unbelievably small radius of curvature could be avoided if only one factor of $(1+z)$ were to be used rather than two, from which it would follow that the *number effect* in the path-length dilution of the photons would not occur, meaning no expansion.

This astonishing conclusion would not be reached today even using the same observational $N(m)$ data, i.e. even if it were assumed that the 1934 apparent magnitude scale was correct. First, Hubble's $K(z)$ correction was based on a blackbody spectrum of temperature 6000 K, whereas the real energy distribution is not a blackbody, and further the color temperature is much smaller (Greenstein 1938). In addition, Hubble mistakenly had no bandwidth term [$2.5 \log(1+z)$] in his $K(z)$ correction. Second, Figure 2 shows that the correct $m(z)$ equation put into the $V(z)$ relations gives much too small a dependence of $N(m)$ on q_0 to measure the space curvature in this way. Although an adequate comparison of Hubble's (1936b) analysis with the modern theory of the standard model has not yet appeared, it is believed that even the sign of his correction term to remove the uncomfortably small radius of curvature is opposite to what we would apply today. A rediscussion of Hubble's analysis in modern terms would be of considerable historical interest.

5.3.2 RECENT GALAXY COUNT DATA AND ANALYSIS The extensive Lick Survey by Shane & Wirtanen (1950, 1967, and prior references), summarized by Shane (1975), began the modern work on the surface galaxy distribution. This survey added a point at $m_{pg} = 19.0$ to the $N(m)$ data, but most importantly it began to show the true fine structure of the surface distribution. The first striking evidence for filaments (anticipated, to be

sure, by Shapley's extensive Bruce telescope survey to 17 mag discussed in many issues of the Harvard Circulars and Bulletins in the 1930s and 1960s) was found by Seldner et al. (1977, Plate I). This was the beginning of the current emphasis on sheets and voids in the three-dimensional spatial galaxy distribution, discovered by Tift & Gregory (1976), Chincarini & Rood (1976), and especially Gregory & Thompson (1978, their Figure 2). These early results are reviewed in these volumes by Oort (1983).

The existence of the sheets and voids (cf. Kirshner et al. 1981, Haynes & Giovanelli 1986, de Lapparent et al. 1986) calls into question the very validity of the count-volume test for measuring the spatial curvature. On the scale of 100 Mpc, the distribution of galaxies is clearly not homogeneous *in detail*. However, it is precisely the necessity of this exact detail that is important if the *slight* deviations of $V(z)$ from Euclidean volumes can, even in principle, be found.

The existence of local inhomogeneities at all redshifts is demonstrated by pencil-beam surveys of redshift distributions, i.e. the number of galaxies in a *complete sample* at redshift z in dz in the magnitude interval dm at m . The theoretical expectation of this distribution is predicted directly by the appropriate sums in the m , $\log \pi$ table solutions of Equation 38, as described in Section 5.2 and by Binggeli et al. (1988, Section 1.2.2) in this volume. Preliminary observational data from two independent pencil-beam redshift studies by Ellis (1987, his Figure 6) and by Koo & Kron (1987, their Figure 1), although clearly showing the voids, have upper-envelope distributions $N(z)$ that are well defined for each data set. This might be used to justify a belief that if averages are taken over sufficiently large areas, the small-scale sheet and void fluctuation distribution will cancel out *exactly*, leaving only a spatial curvature signal. This optimistic view keeps alive the hope for a geometrical solution to the Gauss-Schwarzschild experimental methods to find kc^2/R^2 that we have been discussing. Yet it seems that this approach, in view of the very great inhomogeneities on 100-Mpc scales, is looking more and more like an optimistic climb to the summit of Everest without proper equipment. Yet to remain in the valley is to miss the chance to view the ineffable scene from the summit, on the off chance of reaching it.

In this spirit, first results of many deep-count surveys are now in the literature. Ellis (1987) has reviewed the counts in the (near) B photometric band determined by seven research groups. Differences in the absolute value of $N(m)$ between these various independent surveys exist at the level of a *factor of about 2* at $m \sim 21$ and fainter. It is not yet known if this is due to differences (errors) in the magnitude scales used by the various observers or to real differences between the regions surveyed. To date, the

areas in each survey have necessarily been very small owing to the enormous problem of data reduction of charge-coupled device (CCD) frames between $B \sim 23$ and 26.

On the assumption that the grand average will produce an adequate approximation to homogeneity, so that the data can be compared with the $N(m, q_0, E)$ predictions of the last section, Yoshii & Takahara (1988, their Figure 8) combined the seven surveys [Jarvis & Tyson (1981), Shanks et al (1984), Peterson et al. (1979), Kirshner et al. (1979), Kron (1980a,b), to which can be added Ciardullo (1986), as in Ellis (1987, his Figure 2), and Yee & Green (1987)]. Their diagram showing the differential $A(m)$ counts is reproduced here as Figure 3. Superimposed are the theoretical $A(m, q_0, E)$ curves as calculated by Yoshii & Takahara by a method only briefly explained, but one that appears to be equivalent to what we have given in the last section. In their calculations they used the luminosity evolution function $E(t)$ (their Figure 2) derived by Arimoto & Yoshii (1986, 1987), together with a galaxy morphological mix by Tinsley (1980), similar to that adopted by Pence (1976) and by Ellis (1983).

The most important and best-established result of the major surveys to date is that each data sample shows that $d \log N(m)/dm = 0.6$ for B brighter than 16. This was also shown in detail by Sandage et al. (1972), who summarized earlier data in regions far from the north Galactic anomaly, confirming Hubble and Mayall's (Hubble 1934, 1936b, Mayall 1934) prior central result obtained in the mid-1930s, mentioned earlier. Also highly satisfactory is the observed decrease of the slope for $B > 18$, reaching $d \log A(m)/dm \sim 0.4$ at $B = 20$, which is the predicted value as shown by the theoretical lines in Figure 3. Except for the faint AAT points, which show a factor of 2 excess over the other surveys, the counts and the theory agree moderately well using $q_0 \sim 0.02$ and a galaxy formation redshift of $z_f \sim 5$. This conclusion is the same as that which can be made from Figure 2 of Ellis (1987), where the *no-luminosity* evolution line lies far below the observations, showing that appreciable luminosity evolution is required even at $z \sim 0.4$ to fit the faint count data. The conclusion for luminosity evolution depends, however, on the explicit assumption that the standard model is correct.

It is important to emphasize that no check on the direct predictions of the standard model is available from this test, or indeed from any of the following tests (except for that of the time scale; see Section 9), unless a priori assumptions are made concerning the evolution. It is this aspect of observational cosmology that is so fragile and that poses the most serious questions at the moment concerning the efficacy of the standard tests—with the sole exceptions of (a) the time-scale test, (b) the several inde-

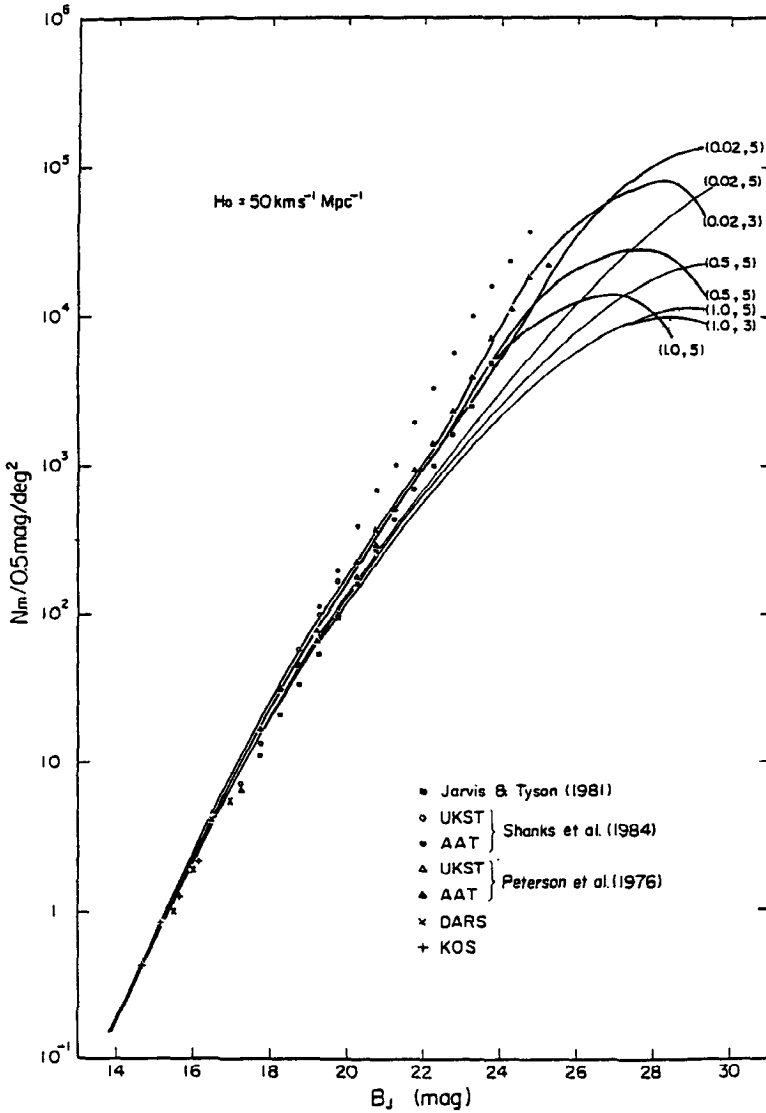


Figure 3 Comparison of predicted $A(m, q_0)$ functions with the observed differential counts (i.e. number at magnitude B_J in magnitude interval ± 0.25 mag) from various surveys. The four heavy lines to the left are for the marked values of q_0 and the redshift of galaxy formation, with luminosity evolution included. The four light lines to the right are the same but with zero luminosity evolution. The relations depend on H_0 only to set the time scale for the galaxy luminosity evolution correction (from Yoshii & Takahara 1988).

Annu. Rev. Astro. Astrophys. 1988.26:561-630. Downloaded from arjournals.annualreviews.org by California Institute of Technology on 04/10/09. For personal use only.

pendent predictions and later discovery of the 3-K Gamow, Alpher, and Herman radiation, and (c) the predictions of nucleosynthesis in the very early phases of the standard model (Boesgaard & Steigman 1985).

Equally good confirmation of the most basic of the $A(m)$ predictions concerning the gross slope of $N(m)$ as a function of magnitude at the bright end comes from the near-red counts in the IIIa F band. Figure 4

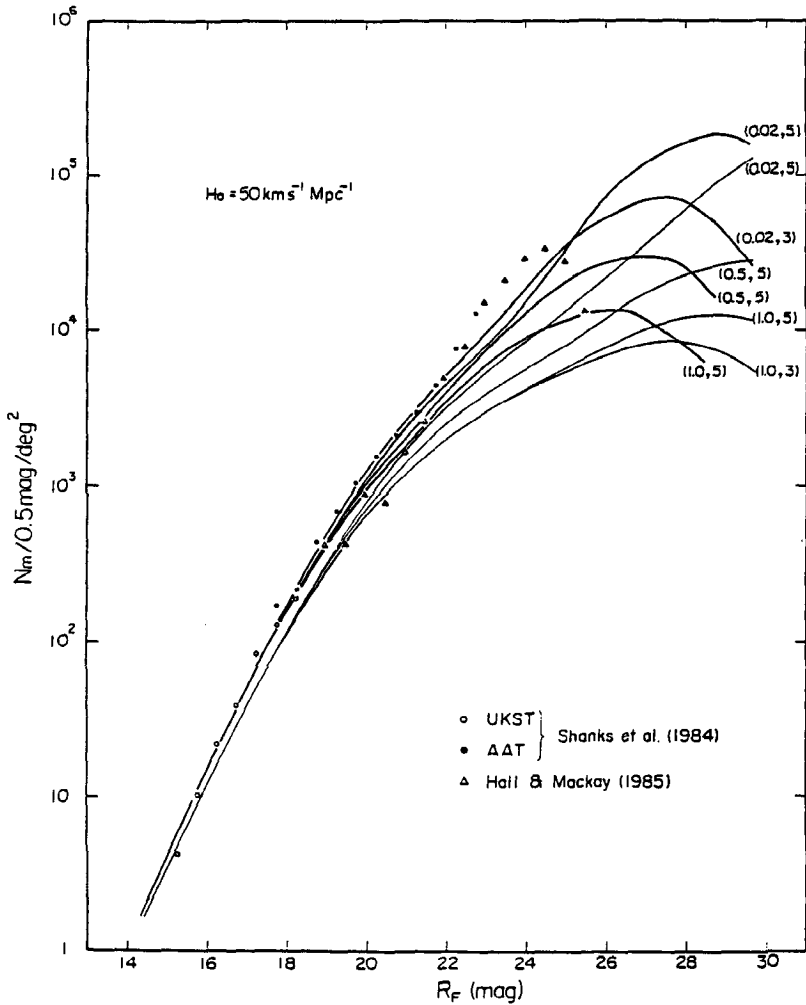


Figure 4 Same as Figure 3, but for near-red magnitudes in the F -band pass (from Yoshii & Takahara 1988).

Annu. Rev. Astro. Astrophys. 1988.26:561-630. Downloaded from arjournals.annualreviews.org by California Institute of Technology on 04/10/09. For personal use only.

(taken from Figure 9 of Yoshii & Takahara 1988) shows the comparison between observations and the model. The data are from Shanks et al. (1984) and Hall & Mackay (1984).

Aside from the gross agreement of slopes, Figures 3 and 4 show again the chief result expected earlier (Brown & Tinsley 1974) that the $A(m, q_0, E)$ differential test, or the $N(m, q_0, E)$ integral test, has little hope of finding q_0 because of (a) the first-order insensitivity to the curvature, and (b) the lack of detailed homogeneity due to the sheet and void properties of the distribution, making the test probably impossible even in principle.

The $m(z)$ test (i.e. the Hubble diagram) entirely avoids this latter problem as long as the inhomogeneities do not induce large velocity perturbations on the Hubble flow at high z , which they certainly do not. The upper limit to such perturbations is of the order $\sim 500 \text{ km s}^{-1}$ given by the noncosmological motion of the Local Supercluster relative to the microwave background [see Tammann & Sandage (1985) for a review]; this is a subject for which a large literature now exists (cf. Dressler et al. 1987). Such perturbations at redshifts $z \sim 0.5$ give velocity perturbations $\Delta v/v \sim 0.0003$, which have negligible effect on $m(z)$, as we now show.

6. THE $m(z)$ HUBBLE DIAGRAM

6.1 *Local Tests for Linearity of the Redshift-Distance Relation*

6.1.1 THE PREDICTION If redshift is due to a real expansion of the geometrical manifold carrying the galaxies with it, the form of the velocity field must be isotropic and linear if space is isotropic and homogeneous. There are many ways to prove this. One of the most straightforward is to consider a triangle. If, upon expansion, the triangle is to be similar to itself, it follows directly that the velocity v_i of any number of points along the sides of the triangle at distances r_i from any arbitrary point must be

$$v_i = H(t)r_i. \quad 40.$$

Otherwise the sides of the triangle will not expand with the same proportionality ratio. The factor $H(t)$ sets the scale of the velocity field at time t .

A linear velocity field has two fundamental properties:

1. The form and the scale of the field are invariant to position, i.e. Equation 40 holds for every point in the manifold upon transferring the origin to it. Hence, the velocity field looks the same from every vantage point, i.e. the ultimate democracy.
2. Upon reversing direction of the velocity vectors to form a *contracting* field, all points arrive at the origin at the same time, i.e. points twice as

far away as others have twice the velocity, hence *equal travel time* to any arbitrary point. And because *all* points are equivalent, all points arrive at all other points together. There is no center of the expansion. All points *have always been* the center.

From these two properties it was early expected that the velocity-distance relation for any reasonable model of an isotropic, homogeneous universe (in the large) must be linear if redshift is a true expansion of the manifold. Note also that the direct prediction of the $m(z)$ relation in the standard model (Equations 33 and 34), using $m - M + 5 = 5 \log r$, gives $cz = H_0 r$ in the $z \rightarrow 0$ limit, which is Equation 40; this provides another way to prove that linearity is a prediction of the standard model.

6.1.2 THE DATA FOR SMALL z For light travel times that are small compared with the age of the Universe, the World picture is nearly the same as the World map, in Milne's (1935) useful language. The light travel time can be neglected for small-enough redshifts.

In the search for the form of the expansion law, the relevant redshift regime in which to exploit this circumstance unencumbered by the non-simultaneity of the observations is $z \leq 0.2$.

Four claims are extant in the literature concerning the dependence of redshifts on distance in the World map. Only one of the following is correct.

1. The relation is linear everywhere, at all distances and at all times. The standard model requires it. We argue herein that the data demand it.
2. The relation is approximately quadratic *locally* (i.e. to $cz \approx 4000$ km s^{-1}); thereafter it becomes linear (de Vaucouleurs 1958, 1972, de Vaucouleurs & Peters 1986, their Figures 2a,b; Giraud 1985, 1986a,b, 1987).
3. The relation is quadratic everywhere (Segal 1975, 1981).
4. The relation is exponential as $1 + z = \exp(HrR/c)$ in the speculation of tired light [LaViolette 1986; see also Pecker & Vigier (1987) for a review].

In his discovery paper, Hubble (1929) claimed a linear relation only quite locally, being aware of de Sitter's (1917) *quadratic* prediction [cf. Sandage (1975b) for a history]. Hubble's final sentence of this first paper was a cautious "and in this connection it may be emphasized that the linear relation found in the present discussion is a first approximation representing a restricted range in distance." His idea evidently was that he might only be observing a linear (tangent) approximation at very small r to the de Sitter $v \sim r^2$ prediction, which might become evident at larger distances.

To test this, Humason (1931) began redshift measurements at Mount

Wilson of bright E galaxies in clusters and found, even at this early date, values as large as $cz \sim 20,000 \text{ km s}^{-1}$ for a cluster in Leo. With these new data, combined with estimates of apparent magnitude, Hubble & Humason (1931) extended the original velocity–apparent magnitude relation approximately twentyfold in distance within two years of the initial discovery.

The slope of the redshift–magnitude relation was found to be 5 to within the errors, proving beyond doubt that the velocity–distance law is linear. However, in 1931 there were only 8 clusters involved in the test. By 1936, Hubble (1936a) and Humason (1936) had increased the data base to 10 clusters reaching $cz = 42,000 \text{ km s}^{-1}$, with the same result. Hubble's (1953) last discussion, in his Darwin lecture, still had only 11 clusters, but the data now reached to $z = 0.2$, which was the largest redshift Humason could measure, even with the early use of the Palomar 200-inch reflector with photographic detection. The result again proved linearity, but the data sample was still small and the photometric measurements had been made using only photographic techniques. The final phase of the initial proof of linearity was the summary paper of HMS, which used new data on 18 clusters. However, the universality of the phenomenon was more inferred than established because there were still so few clusters.

Early claims of nonlinearity (cf. Hawkins 1962) used the HMS data on *field* galaxies taken from *flux-limited* samples and failed to correct for sample bias. Modern discussions of local nonlinearity, some of which are referenced earlier in this section, also use field galaxies. Because the luminosity function of field galaxies is considerably broader than for first-ranked cluster galaxies, some conclusions from these field galaxy studies have been criticized as due to insufficient corrections for the selection bias. Discussions of the bias have been given by Teerikorpi (1975a,b, 1984, 1987), Bottinelli et al. (1986, 1987, 1988), and Sandage (1988a,b). The principal consequences of bias neglect have been (a) an incorrectly high value of the Hubble constant and (b) a false belief that the consequent calculated variation of H_0 with distance, increasing outward, is real (Section 9).

Discussion of the bias effects in the flux-limited RSA catalog became possible when the redshift coverage of that catalog became complete, following the finalization (Sandage 1978) of the Humason & Mayall (HMS) redshift program. The bias in the field galaxy sample was shown directly (Sandage et al. 1979), and the apparent increase of H_0 with distance was demonstrated to be an artifact, caused by assigning a fixed $\langle M \rangle$ value to all galaxies in the flux-limited sample. These selection effects are severe enough that study of the form of the redshift–distance relation using field galaxies is dangerous owing to the necessary corrections that are difficult

to make accurately. For this reason, study of the $m(z)$ relation to test for linearity was begun in the early 1970s using *cluster* and *group* samples. The photometry in these studies was done by photoelectric techniques; the results, reported in a series of papers (Sandage 1972a,b,c, 1973a,b, 1975a, 1986, Sandage et al. 1972, Sandage & Hardy 1973), again confirmed the linearity of the local velocity-distance relation.

The principal conclusion of the work was that the leading term of $5 \log cz$ in the theoretical prediction of Equation 34 is fully confirmed. The standard model does, then, pass this most elementary of its predictions.

6.2 The Hubble Diagram at Large Redshifts

Determination of the second term involving q_0 in Equations 33–35 was the principal motivation for extending the Hubble $m(z)$ diagram to the largest possible redshifts. The correction is of first order in z (cf. Equation 34) and hence is a large effect. To see how large, recall the special cases of $q_0 = 0$ and $q_0 = 1/2$ for Rr_0 of Equations 22 and 26, which (when put into Equation 32 for the flux) give the closed expressions

$$m_{\text{bol}} = 5 \log \left[z \left(1 + \frac{z}{2} \right) \right] + \text{constant} \quad \text{for } q_0 = 0, \quad 41.$$

and

$$m_{\text{bol}} = 5 \log [2(1+z - \sqrt{1+z})] + \text{constant} \quad \text{for } q_0 = 1/2, \quad 42.$$

where the constant is the same in both equations. These are special cases of the general equation (Equation 33). If, then, we could observe to $z = 1$ and determine m_{bol} , the magnitude difference between the $q_0 = 0$ and $q_0 = 1/2$ cases would be $\Delta m_{\text{bol}} = 0.54$ mag, the $q_0 = 1/2$ case being brighter, assuming no luminosity evolution in the look-back time.

Early studies aimed to determine q_0 this way were reviewed by Peach (1970, 1972). Special programs to extend the Hubble diagram to very large redshifts were begun by Gunn & Oke (1975), Sandage et al. (1976), Kristian et al. (1978), Hoessel (1980), and Schneider et al. (1983a,b), and these studies reached redshifts of $z = 0.5$ (excluding the radio galaxies). Very much larger redshifts for cluster galaxies have become available by including radio sources in the sample [see Spinrad (1986, and references therein) for a review].

6.2.1 CORRECTIONS TO THE MAGNITUDES FOR THE HUBBLE DIAGRAM

Several technical corrections are needed before Equation 35 can be used to obtain q_0 .

1. *The aperture correction* must be made to reduce the photometric

measurements to either a standard isophote (Sandage 1975a, Table B1) or to a standard metric diameter (Sandage 1972a, Table 3). The first method requires knowledge of the isophotal radius such as that of Holmberg (1958), or the D_s of HMS (appendix A) estimated from the original Palomar Sky Survey blue plates, or $D(0)$ of de Vaucouleurs et al. (1977; hereinafter RC2). The argument of the generally adopted standard curve (Sandage 1975a, Table B1) is $\theta/2.5 D(0)$. The second method, using a standard *metric* diameter, depends on q_0 , because the space curvature is needed to calculate the $r(z)$ function (Equations 29 and 30 of Section 3.1), but the q_0 dependence of the final magnitude correction is nearly negligible, provided that the chosen standard radius is large enough. This is shown by the metric aperture corrections calculated by Kristian et al. (1978) for $q_0 = 0$ and $q_0 = +1$ separately. The final magnitudes differ by less than 0.1 mag between the two q_0 models, even for $z = 0.5$, belying the criticism of Segal (1976) concerning a circular argument that he implies leads to a lack of convergence of the method and therefore to an incorrect conclusion concerning the linearity of the velocity field.

Gunn & Oke (1975) use the same precept for their aperture corrections by reducing their data to a standard aperture that corresponds to a metric radius of ~ 16 kpc (for $H_0 = 60$, $q_0 = 1/2$). That of Sandage is at ~ 86 kpc ($H_0 = 50$). The Oke-Gunn radius is so small, however, that the dependence of their aperture corrections on q_0 , done this way, is much larger than for the correction used by Sandage (1975a) and by Kristian et al. (1978).

2. *Galactic absorption* corrections are controversial, depending on the assumption of either large (de Vaucouleurs & Malik 1969) or near-zero (Sandage 1972b, Section III) absorption at the Galactic pole. Galaxy counts have always been interpreted as requiring absorption at the pole, even as high as $A_B \sim 0.5$ mag (Hubble 1934, Shane & Wirtanen 1954, 1967, Noonan 1971, Holmberg 1974, Heiles 1976), but Noonan makes the point that counts below $b = 45^\circ$ need not be related to counts at the pole if the Galactic absorption is patchy [small clouds, such as scattered summer cumulus, with which the zenith is mostly clear but the horizon is not due to the highly nonlinear areas (on the sky) at equal intervals of the zenith angle intervals].

The absorption-free polar cap model of McClure & Crawford (1971) is consistent with galaxy colors as a function of latitude (Sandage 1973a, Sandage & Visvanathan 1978, Section VI), leading to the absorption correction of $A_B = 0.13 (\csc b - 1)$ for $|b| < 50^\circ$ and $A_B = 0$ for $|b| > 60^\circ$, but smoothed for $|b| = 50\text{--}60^\circ$ to avoid a step. This correction was used in the Mount Wilson series of papers on the $m(z)$ Hubble diagram mentioned in Section 6.1.2.

3. *A cluster richness* correction has been derived by correlating the

population of clusters with the magnitude deviations of individual first-ranked cluster galaxies from the $m(z)$ ridge line. Early indications that the change in M_v (brightest) with cluster richness was negligible at the ± 0.1 mag level (Peach 1969, Sandage 1972b, his Figure 8) had to be modified when a prior correction was made for contrast effect (Section 6.2.2); this correction gave a measurable trend of M_v with a range of 0.4 mag over the Abell richness classes from 0 to 4 (Sandage & Hardy 1973). More complete data (Sandage et al. 1976, their Figure 3; Schneider et al. 1983b, their Figure 3) reduce the amplitude of the effect for first-ranked galaxies to ~ 0.3 mag over the same richness range. This is so small as to keep the problem unsolved as to whether the $\Delta M = f(\text{richness})$ data are consistent with (a) a stochastic sampling of the luminosity function or (b) special formation conditions of brightest cluster galaxies. A large literature exists on each side of the issue. Early papers by Peebles (1968, 1969), Peach (1969), and Peterson (1970a,b) came to different conclusions. New data on sparse groups (Sandage 1976), when combined with all existing data on great clusters, showed that the variation of the absolute magnitudes of first-, second-, and third-ranked cluster galaxies with richness was too shallow to be explained by the bright-end slope to $\phi(M)$. The opposite conclusion was stated by Geller & Peebles (1976), although their calculations clearly do not fit the data (their Figure 9). Schechter & Peebles (1976), admitting this, then attributed the lack of agreement between a statistical theory and the data to a Malmquist-like selection effect if the sparse groups were chosen from flux-limited catalogs. Nevertheless, their Figure 5 is an important one for practical cosmology, showing that the richness correction is, in fact, small for rich clusters ($\log N_c^{48} > 1.4$). This makes the *observed* correction (Sandage et al. 1976, their Figure 3) valid, even neglecting the supposed bias that results from using flux-limited samples.

The discussion took on new life with Tremaine & Richstone's (1977) conclusions from the data on the first three ranked galaxies that the special formation condition is marginally favored over the statistical theory. Geller & Postman (1983) concluded the opposite. Hence, the explanation of the $M_i = f(\text{richness})$ correlation appears not yet to be satisfactory. New data are needed on sparse groups, chosen from fainter flux-limited catalogs than those used by Sandage (1975a) or by Huchra & Geller (1982) and Geller & Huchra (1983). Despite this, as just mentioned, the richness correlation for the rich clusters, as determined directly from the observations [by either Sandage et al. (1976) or Schneider et al. (1983b)], *does* give a quite adequate correction of magnitudes to a standard cluster richness.

4. *Bautz & Morgan* (1970) devised a classification system for clusters and groups of galaxies based on the contrast in brightness of the first-

ranked member with fainter cluster members. From a study of magnitude residuals about the mean $m(z)$ ridge line, Sandage & Hardy (1973, their Figure 2) found that the absolute magnitude of the first-ranked galaxy correlated with Bautz-Morgan cluster type—the greater the contrast, the brighter M_1 . A frequent explanation is that “cannibalism” of the first-ranked galaxy on its cluster family has occurred (Ostriker & Tremaine 1975, Ostriker & Hausman 1977, Hausman & Ostriker 1978, Tremaine 1981). Whatever its explanation, the contrast effect seems quite real for first-ranked galaxies. The amplitude of the correction determined by Schneider et al. (1983b, their Figure 3) is similar to that found earlier by Sandage & Hardy (1973, their Figure 2) and is well determined.

The four corrections just discussed (aperture, galactic absorption, richness, contrast), together with the K redshift dimming (Section 4.2), give the luminosity data needed for Equation 35 when applied to the measured magnitudes of first-ranked galaxies. The resulting $m(z)$ Hubble diagram, plotted with the evolution effect $E(z)$ taken to be zero, is reproduced here as Figure 5, taken from Sandage & Hardy (1973).

The line in Figure 5 has the theoretical slope of 5 required by a linear redshift-distance relation. The scatter about this line is not a function of redshift. It has $\sigma(M_1) = 0.28$ mag as the intrinsic dispersion of first-ranked cluster galaxies using “fully corrected” magnitudes, showing that such galaxies are among the best standard candles known as distance indicators.

6.2.2 ATTEMPTS TO DETERMINE q_0 IN OPTICAL WAVELENGTHS In order to exploit the standard candle nature of first-ranked cluster galaxies, attempts have been made to determine q_0 from Equation 35 by (a) obtaining data to very large redshifts and (b) estimating the evolutionary correction $E(t)$ from stellar evolution theory of the changing HR diagram with time, already described. The two early attempts using the Hubble diagram in optical wavelengths by Gunn & Oke (1975) and by Sandage et al. (1976) and Kristian et al. (1978) (discussed earlier) reached only $z = 0.75$, which, from Equations 39 and 40, gives a wedge of only $\Delta\text{mag} = 0.4$ mag on the problem between the $q_0 = 0$ and $q_0 = 1/2$ cases. Because of the smallness of the effect to this small limiting redshift, it is not so surprising that the formal solutions given by the two groups of $q_0 = 0.33 \pm 0.7$ or $q_0 = -1.27 \pm 0.7$ by Gunn & Oke and $q_0 = 1.6 \pm 0.4$ by Kristian et al. (and later $q_0 = -0.55 \pm 0.45$ by Hoessel et al. 1980) are as close as they are. Furthermore, the solutions mean nothing until the $E(t)$ correction for luminosity evolution is applied. This term is large in BVR wavelengths. Because it is expected to be small in the near-IR, major studies were begun in the early 1980s in this wavelength region.

6.2.3 THE HUBBLE DIAGRAM IN THE NEAR-INFRARED The two principal

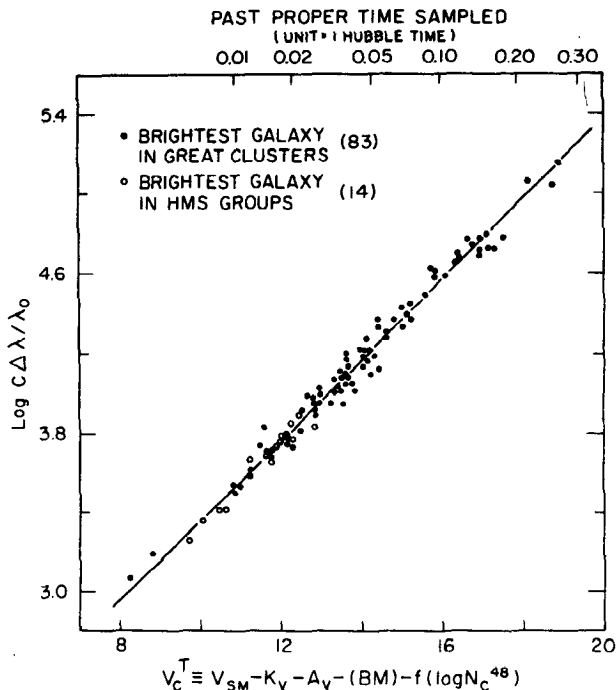


Figure 5 The $m(z)$ fully corrected Hubble diagram for first-ranked E galaxies in clusters. Corrections to magnitudes are made for K dimming, absorption due to the Galaxy, the Bautz-Morgan contrast effect, and cluster richness (from Sandage & Hardy 1973).

advantages of observations in the near-IR for large redshifts are (a) that the K correction is appreciably smaller than in the B and V wavelengths, and (b) that the $E(t)$ evolution term is insensitive to starburst evolution (termed active evolution by Lilly & Longair 1984). Furthermore, its amplitude for passive evolution (i.e. the gradual evolution of the HR diagram of an old coeval population with time) is also much smaller in the K band than in the UBV or R bands.

A pioneering advance in K -band photometry was made by Grasdalen (1980) and by Lebofsky (1980), who gave the first $m(z)$ Hubble IR diagram. Lebofsky (1981), by including radio galaxies, reached $z = 1.18$ and obtained a value of $q_0 = -0.05 \pm 0.30$ for $z < 0.5$, where the $E_K(t)$ evolution term was taken to be zero. A hint for mild evolution for $z > 0.5$ was found even in these early data. More extensive observations (Lebofsky & Eisenhardt 1986) continued to show evidence for mild luminosity evolution, consistent with Tinsley's (1978) predictions.

Lilly & Longair (1982, 1984) greatly extended the sample using radio galaxies, reaching $z > 1$ with a substantial number of objects. They concluded that $q_0 \sim 0.5$ if $E_K(z = 1) = 1$ mag, obtained from the (apparent) value of $q_0 = 3.7$ (their Figure 8). They countered a criticism concerning the use of radio galaxies for their survey by showing no difference in the $m(z)$ relation between strong radio sources (using 3C sources, and hence with radio flux greater than 9 janskys) and weaker 1-jansky sources (Lilly et al. 1985).

These near-IR data gave the first convincing evidence for luminosity evolution in the look-back time to $z = 1$. A summary of the K data, with the $m(z, E)$ model lines superposed, is given by Yoshii & Takahara (1988, their Figure 4), shown here as Figure 6. The conclusion from these data is that no model with $E = 0$ for $q_0 < 1$ fits the near-IR Hubble diagram data, and therefore that evolution is required, taking the data as they stand.

6.2.4 EVIDENCE FOR LUMINOSITY EVOLUTION FROM THE V-BAND HUBBLE DIAGRAM Even more powerful evidence that the evolution term $E(z)$ has been detected comes from the work at very large redshifts by Djorgovski et al. (1985), summarized by Spinrad (1986) and by Spinrad & Djorgovski (1987) using radio galaxies, reaching $z = 1.8$. Figure 7 is their summary Hubble diagram in V , in which data from a number of authors are combined. The V magnitudes are as observed, corrected only for aperture effect (no K correction). Theoretical lines from Equation 35 are shown [a K term and $E(t)$ evolution according to various Bruzual models are put into the theoretical model lines, rather than corrections to the observations]. The conclusion is that the data for $z > 0.8$ cannot be fit by *any* q_0 value in the no-evolution case [i.e. $E(t) = 0$], whereas a good fit is obtained with a Bruzual evolving model with $q_0 = 0$ and $H_0 = 50$.

A different representation of a subset of these data is shown in Figure 8, again taken from Yoshii & Takahara (1988, their Figure 3). As before, the V magnitude is corrected only to the standard metric size for aperture effect. Again the K redshift dimming and $E(t)$ corrections are put into the theoretical lines that show q_0 and the redshift of galaxy formation in the evolving models; these are shown as the four heavy lines to the left ($H_0 = 50$ km s⁻¹ Mpc⁻¹ is assumed so as to set the time scale of the evolution in the look-back time). The three lighter lines to the right are for no evolution for the $q_0 = 1, 0.5,$ and 0.02 cases, none of which fit the data for $z > 0.5$. The assumed $E(t)$ evolution, as explained earlier, is that given in Figure 2 of Yoshii & Takahara (1988), based on work by Arimoto & Yoshii (1986, 1987).

The conclusion from Figures 7 and 8 is that evolution must be invoked

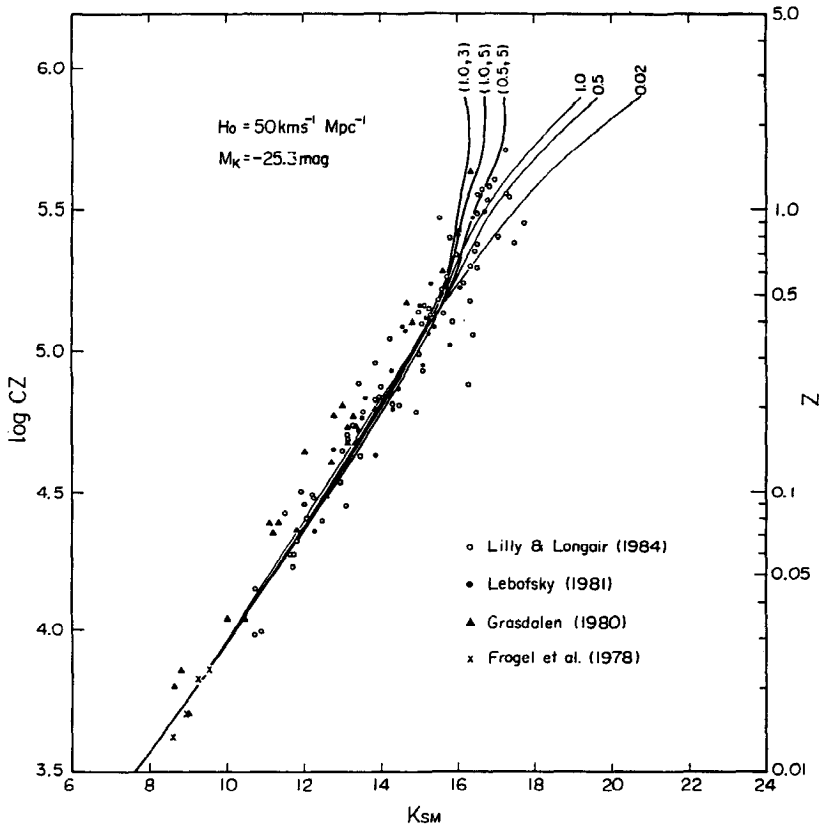


Figure 6 The near-IR Hubble $m(z)$ diagram using K -band magnitudes corrected to a “standard metric” aperture size. The three left-hand theoretical curves are the expected relations (Equation 35) for $q_0 = 1.0$ and $q_0 = 0.5$ using the relevant $E(t)$ evolution corrections. The redshift of galaxy formation is marked ($z = 3, 5,$ and 5). The three right-hand curves are for the marked q_0 values with no evolution correction. K redshift corrections have been applied to the theoretical curves rather than the magnitudes (from Yoshii & Takahara 1988).

if the prediction of the standard model (Equation 35) is to be claimed to be verified. This is a second demonstration (the first being the observed excess number counts over the predictions in Figures 3 and 4) that the observations cannot be used to confirm the simplest standard model because we must “save the phenomenon” by adding evolution. Of course, evolution *is expected* and, indeed, must be found if the standard model is to be correct because the mean age of the galaxies is required to be a function of redshift. However, it is important to note that the argument is

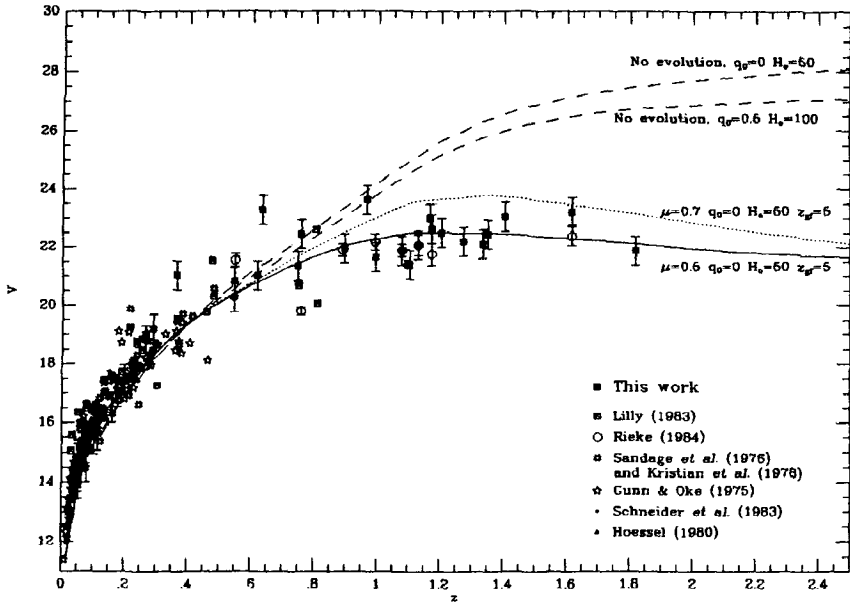


Figure 7 The $m(z)$ Hubble diagram (plotted differently from Figure 5, with V magnitude as ordinate and linearly with z) extended to large redshift. Predicted theoretical $m(z)$ lines for various q_0 values and evolutionary corrections (Bruzual models) are shown. The K corrections have been applied to the theoretical curves (from Djorgovski et al. 1985).

circular if we use the standard model predictions to prove that evolution has occurred without having a priori proof that the standard model is correct. It is, then, incumbent on the claimer to show a *consistent* series of needs for look-back time evolution, independent of the $N(m)$ and $m(z)$ theoretical relations that themselves depend on the standard model. Stated differently, “The standard model requires evolution; and indeed, if evolution is left out, the model doesn’t [and shouldn’t] fit the data. On the other hand, to test the model *with* evolution we’d need an *independent* theory of the effects of evolution, which we don’t yet have” (D. Layzer, private communication, 1988).

7. NONGEOMETRICAL EVIDENCE FOR EVOLUTION IN THE LOOK-BACK TIME

Due to this circularity of the argument for luminosity evolution, we seek evolutionary tests that are independent of the geometry, i.e. of q_0 . Currently, such tests are of two kinds. In the first we look for changes in

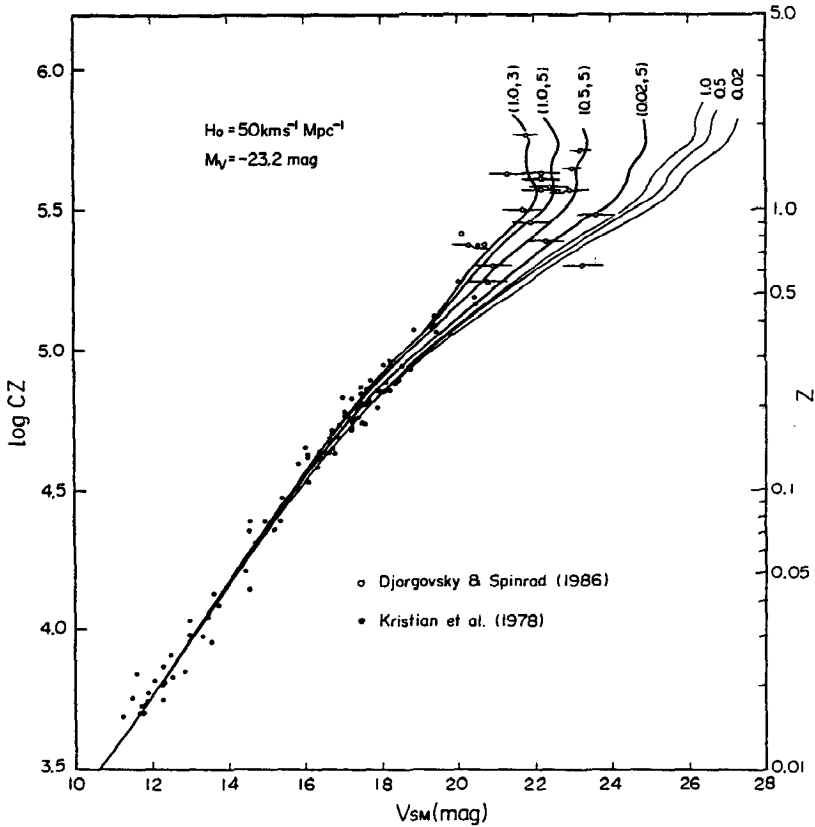


Figure 8 Same as Figure 6, but for V -band magnitudes (summary diagram from Yoshii & Takahara 1988).

the shape of the spectral energy distribution for “standard” galaxies (i.e. of particular Hubble types) at different redshifts. In the second, differences in the expected morphological mix in particular environments at different redshifts are queried for possible evolutionary information. A comprehensive review is given by Kron (1982).

7.1 Changes in Spectral Energy Distribution With Redshift

7.1.1 BROADBAND COLORS Calculations of time-variable evolution were possible as soon as it was realized that the HR diagram could be explained by evolutionary tracks off the main sequence rather than up it, and especially that the Trumpler (1925) cluster classification was an age

sequence (Sandage 1953, 1957, 1958). Empirical evidence for the change of color with time of stellar systems that had coeval star formation was set out from galactic cluster data (Sandage 1963, his Figure 7). The $B-V$ colors of the *integrated* light from any given cluster was found to correlate well with its age over the age range from 10^6 to 10^{10} yr.

The effect was successfully modeled by Searle et al. (1973) in what was one of the first papers on theoretical galaxy evolution, a subject that has developed into the current flood of detailed studies, often reviewed [e.g. IAU Symposia Nos. 79, 92, 104, and 124, and the Erice workshop on galaxies at high redshift (Kron & Renzini 1988)].

A principal result of the early work was to show how very slow the color evolution is with time for old stellar systems. The "observed" rate from galactic clusters is $\Delta(B-V)/\Delta t \simeq 0.03$ mag per 10^9 yr at age $\sim 10^{10}$ yr (Sandage 1963, his Figure 7). This observational result is the same as the theoretical calculation given earlier by Crampin & Hoyle (1961), who asked what the colors of M67 would be at earlier ages. The very shallow color dependence with old age is also a characteristic of all subsequent reasonable galaxy evolution models, no matter what their level of sophistication (cf. Quirk & Tinsley 1973, their Figure 1; Huchra 1977, Larson & Tinsley 1978, their Figure 2; Bruzual & Kron 1980, and references therein).

This expected rate of $B-V$ change (in the rest wavelength frame) with look-back time can be transformed into a function of z using Equations 36 and 37, which relate z with the evolutionary time for the special cases of $q_0 = 0$ and $q_0 = 1/2$. The age of the $q_0 = 1/2$ model is 13×10^9 yr if $H_0 = 50$. Redshifts of 0.2, 0.5, and 1.0 have look-back times of 3.1×10^9 , 5.9×10^9 , and 8.4×10^9 yr, respectively, in this case. Hence, no color evolution larger than $\Delta(B-V) \simeq 0.1$ mag is expected for E galaxies until $z > 0.2$, after which color effects larger than this should appear.

This expectation is confirmed. Figure 9 shows the observed $B-V$ colors of first-ranked E galaxies to redshifts as large as $z = 0.2$ compared with the predicted color of a standard E galaxy redshifted through the B and V photometric bands. No color evolution has yet occurred. Only after extension to larger redshifts and to the $V-R$ color does some color evolution begin to occur, as expected (Kristian et al. 1978, Djorgovski et al. 1985). The available $V-R$ data are shown in Figure 10. The *no-evolution* case (the simple K correction applied alone as described in Section 4.2) does not fit the data.

These first attempts to find color evolution used broadband photometry of first-ranked cluster E galaxies. In the work of Kristian et al. (1978) the cluster sample was taken from the list of classical clusters known to HMS and from the Abell (1958) catalog, to which they added their sample of large-redshift clusters ($z \sim 0.2-0.7$) found in a special search using IIIaJ

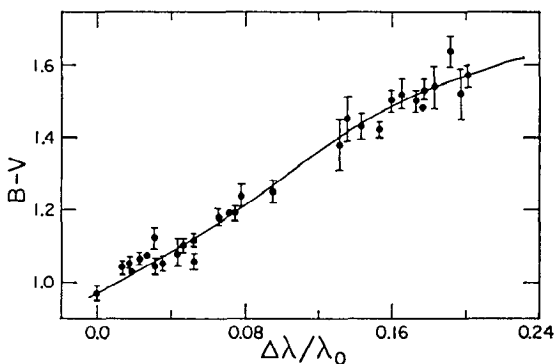


Figure 9 Observed and predicted $B-V$, redshift relation for first-ranked E galaxies (from Oke & Sandage 1968).

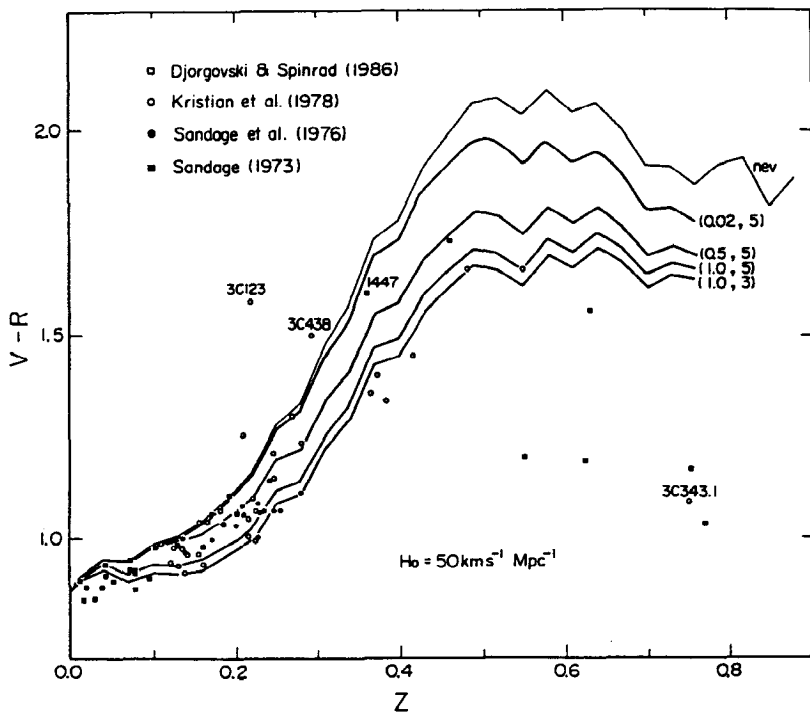


Figure 10 Same as Figure 9 for $V-R$ colors. The theoretical curves are for various q_0 and redshift formation values using adopted luminosity evolutionary corrections. The upper curve is for no evolution of the spectral energy distribution. Evolution is clearly required by the data at high redshift (from Yoshii & Takahara 1988).

photography with the Palomar 48-inch Schmidt telescope (unpublished). A deeper special search by Gunn et al. (1986) lists the most distant cluster candidates yet known, found in a similar survey employing both the Schmidt and the 200-inch Hale reflector.

From an intensive study of Kron's distant cluster 0016+16 ($z = 0.54$), Koo (1981) used *UBVI* broadband photometry to demonstrate the existence of many red galaxies that have the nearly normal colors of nearby E/S0 galaxies, redshifted without appreciable color evolution. Koo cited the results as a counterexample of the Butcher-Oemler effect (Section 7.2.1). However, he later joined with Ellis et al. (1985) to show from intermediate-band six-color photometry that the mean energy distribution of the E/S0 candidates in this cluster was "significantly bluer than the present day equivalent (galaxies) at ultraviolet wavelengths," and therefore that *passive evolution* of the spectral energy distribution probably had occurred over this look-back time.

However, the effects are small. Contradictory evidence in the field (Koo & Kron 1988a,b) and in other clusters suggests that the rate of evolution may not be the same in all E/S0 galaxies in all environments at any given redshift (Ellis 1988). If so, the evolutionary term $E(t)$ in Equation 35 *would not be a unique function of look-back time, even for any given Hubble type*. This evolutionary correction to the $m(z)$ Hubble diagram would then be a *stochastic variable*, and the hope to find q_0 by this direct route would again recede as it has so often before.

7.1.2 DETAILED SPECTRAL ENERGY DISTRIBUTIONS *Broadband* colors disadvantageously integrate over important details of the spectra that should betray any evolution more sensitively. Oke (1971) obtained spectra of three moderately high-redshift galaxies ($z = 0.20, 0.38, 0.46$) and found no evidence for evolution in the green and red, but he had no fiducial spectrum in the UV with which to compare over this more sensitive region. Wilkinson & Oke (1978) extended the sample to 56 galaxies and again found no effect larger than $\Delta(B - V) = 0.04$ mag (if that) to the look-back time corresponding to $z = 0.46$. They attributed their failure to detect even a small expected effect to variations in the intrinsic properties of the sample galaxies—they are not all perfect templates of an ideal standard.

The large sample size of the Wilkerson-Oke study gives considerable weight to their conclusions. However, there are hints of evolution in the SEDs of specially selected samples. Spinrad (1986, his Figures 12 and 13) shows that the mean SED of two giant E galaxies at $z = 0.2$ is redder than Schild & Oke's (1971) standard SED for first-ranked E galaxies. He also finds that the mean spectra of three giant E's at $z = 0.75$ is substantially bluer in the more sensitive ultraviolet than is the standard. But again,

contradictory evidence in field galaxy samples [see Koo (1988b) for a review] is that little or no color evolution exists in average samples to $z \sim 0.4$. However, evidence discussed in the next two sections suggests that the presence or absence of evolution may depend on the nature of the sample, and that the effects (if present) are likely to be hidden among stronger selection biases.

7.1.3 THE 4000-Å BREAK Bruzual (1983a, his Figure 4), following Spinrad (1977, 1980), presented observational evidence and theoretical models of the change in the 4000-Å spectral discontinuity with time for different star formation rates. The size of this spectral “break” is a moderately sensitive function of the spectral type of the main sequence termination point (Bruzual 1983a, his Figure 3; Hamilton 1985, his Figure 6). It is also known to be sensitive to metallicity at a given temperature, being the chief blanketing index for the UV excess given by $\delta(U - B)$ (or m_1) that measures $[\text{Fe}/\text{H}]$ for F and G subdwarfs (Roman 1954, Sandage & Eggen 1959, Strömberg 1966). For these two reasons (age and metallicity) the break strength is expected to change with look-back time in some models of evolution of standard galaxies of a given Hubble type.

Spinrad’s (1986, his Figure 15) data show a pronounced change of break strength with redshift for E galaxies in clusters *chosen without regard to galaxy color*, i.e. simply an “average” galaxy, wherever it could be found. The break change with z observed by Spinrad agrees well with one of the calculated models by Bruzual.

However, in a remarkable development, Hamilton (1985) applied a rigid color selection criterion for a galaxy sample that he used to study the redshift dependence of the break amplitude. In a massive four-color survey that covered 4 square degrees, composed of eight high-latitude fields, Hamilton picked the reddest galaxies in the sample, using color-color plots. There was no appeal in the selection to cluster membership because the selection criterion was blind to any fact but reddest color. The redshift range of Hamilton’s sample was $z = 0 - 0.8$. *No* change of break amplitude was detected at least to $z = 0.6$, in contrast to Spinrad’s result for his more “average” sample.

Hamilton’s result shows that very old galaxies exist at $z = 0.8$ that are at least 2×10^9 yr older than the look-back time of $\tau = 8.7 \times 10^9$ yr (if $H_0 = 50$, $q_0 = 0$). He finds no evidence for either recent star formation or for passive evolution of the stellar content of *this sample*. Hamilton’s observed lack of passive evolution is consistent with his models, but it is not in agreement with the models of Bruzual. The data prove that at least *some* normal, nonstarbursting E galaxies exist at large redshift, and that they are *old*.

Does Spinrad's result require evolution for *his* sample? There is no proof in Spinrad's data that his sample is composed of normal ellipticals, rather than Sa, Sb, or Sc galaxies. It is known that these later types have systematically smaller breaks in local galaxies than in local ellipticals [Hamilton 1985, his Table 2 (from the data of Heckman et al. 1980)]. Spinrad's sample of not necessarily first-ranked cluster galaxies may contain these later types. The same reason of mixed morphology might explain the larger dispersion in break amplitude at a given absolute magnitude that was found by Dressler & Shectman (1987) in galaxies in moderately distant clusters but not by Kimble et al. (1987) in local E and S0 galaxies in the Virgo cluster.

The conclusion is that secular spectral evolution in the look-back time to $z = 0.8$ has *not* been shown, beyond doubt, from the break data. As with the broadband data the results are, as yet, marginal, but the potential of the method is great.

7.2 Changes in Morphological Mix

7.2.1 THE BUTCHER-OEMLER EFFECT A new direction for tests of evolution in the look-back time was set out by Butcher & Oemler (1978a,b, 1984a,b) in their studies of the fraction of blue galaxies to the total population of clusters as a function of redshift. They maintain that there is evidence for secular *morphological* evolution in the cores of clusters because the blue to red ratio is a progressive function of redshift, starting at the very low redshift of $z \simeq 0.15$! A large literature has grown covering the effect, coming down on both sides of the issue. The criticisms that seemed most serious to Butcher & Oemler were made by Mathieu & Spinrad (1981) and Dressler & Gunn (1982, 1983) concerning cluster membership, and by Wirth & Gallagher (1980) concerning the proper normalization of the blue-red ratio in nearby clusters. On the other side, confirmation support was given by Couch & Newell (1984), who expanded the sample. These authors also answered a criticism concerning a color bias effect with redshift caused by different K corrections for different morphological types (Section 4), a problem raised by DeGioia-Eastwood & Grasdalen (1980). Furthermore, the effect appears *not* to be present in every cluster; a notable example is the very compact cluster 0016 + 16 found by Kron ($z = 0.54$), as discussed by Koo (1981). A comprehensive discussion of various selection effects that cloud the issue of the reality of the effect is given by Koo (1988a).

7.2.2 THE DRESSLER-GUNN EFFECT In a spectroscopic study of the Butcher-Oemler effect, Dressler & Gunn (1982, 1983) discovered that the percentage of emission-line galaxies in distant clusters was higher than in

control fields at low redshift. A literature has also grown on this subject both for cluster galaxies and now, with the great recent emphasis, for the field [see Ellis (1988) for a review]. Dressler & Gunn's discovery has been interpreted (Dressler & Gunn 1982, 1983, Dressler 1984) as evidence for recent (last $\sim 2 \times 10^9$ yr) star formation in otherwise "dead" E galaxies. This active evolution is different from the slow passive evolution of old stellar systems mentioned before. If the abnormal activity occurs in otherwise dead E galaxies, bursts of star formation must be postulated at the relevant look-back time.

But a word of caution is in order. No morphological information on galaxy types is yet available for the galaxies with active spectra found by Dressler & Gunn. As pointed out by Koo (1988a), Osterbrock's (1984) bias caution may hold the key to explaining the Dressler-Gunn statistics as a selection effect giving a false impression of an emission-line excess in the field. Seyfert galaxies are among the brightest and bluest galaxies in any volume of space. Hence, in any surveys that are flux limited, they will dominate the statistics in numbers appearing to increase in percentage over intrinsically fainter galaxies at faint apparent magnitudes. It remains a problem to determine if this selection bias can affect Dressler and Gunn's conclusion concerning the unexpectedly strong spectral activity as a function of redshift for field galaxies.

However, much additional work supports the reality of the Dressler-Gunn interpretation of recent starburst activity in *some*, but not all, otherwise dead ellipticals in clusters with $z > 0.3$. Ellis (1988) reviews the situation as it appeared in mid-1987. Observations of ~ 100 galaxies in Abell cluster 370 ($z = 0.37$) by McLaren et al. (1988) suggest that UV light from young blue stars has been added recently to only 15% of the E galaxies [the remaining 85% remaining normal, reminiscent of Hamilton's (1985) result]; but in this 15% this is a phenomenon of starbursting that is *unknown* in local E galaxies observed so far with the IUE satellite, which again suggests evolution in the look-back time.

7.3 *Reassessment of the $N(m)$ Count Evidence for Luminosity Evolution at $z > 0.5$*

Faint multicolor photometry of survey fields for the galaxy number count data is beginning to produce data that will eventually tell if the $N(m, q_0, E)$ excess for $m > 21$ is due to luminosity evolution, i.e. to the $E(z)$ term in Equation 35. Ellis (1988) reviews the enigma that the colors become significantly bluer than expected at magnitude fainter than $m_J \sim 21$ (see also Kron 1980a, Hamilton 1985), where m_J is the J -band magnitude. Furthermore, this is just brightward of where the $N(m)$ counts begin to show an excess from the predicted curves (Figure 2), an excess that grows

to a factor of ~ 10 over the model at $m_J \sim 26$. Recall that this excess has been considered to be strong evidence for luminosity evolution.

However, the mean redshift at $m_J \sim 21$ for *field* galaxies is only $z \sim 0.4$, which is so small that no appreciable luminosity evolution is expected in any reasonable galaxy evolution model. This circumstance gives a clue to what is happening. Spectroscopy is not yet available for complete galaxy samples in the critical magnitude range of $m_J > 21.5$ so as to determine the redshift distribution. However, in an initial redshift survey that is complete between $20.0 < m_J < 21.5$, Broadhurst et al. (1987, as summarized by Ellis 1987) found a subset of the complete 200 field galaxy sample that was blue and had strong emission lines. A further subset of these blue galaxies has a slope of $d \log N(m)/dm = 0.6 \pm 0.2$ for the counts, suggesting that they are nearby and intrinsically faint. If the blue galaxies are removed from the complete sample, the slope for the remainder of the counts is $d \log N(m)/dm = 0.34$ rather than 0.44, causing the *excess counts* at faint magnitudes in Figure 3 to disappear. Clearly redshifts for the entire blue subset are required to make a stronger case. However, these data suggest that luminosity evolution for field galaxies at $z \simeq 0.4$ may not be needed to explain the $N(m)$ counts. But if so, one of the stronger cases for evolution would disappear.

7.4 Evolution Inferred From Quasar Counts

Two aspects of the quasar distribution functions $N(m)$ and $N(z)$ give the strongest geometrical evidence for evolution.

7.4.1 SLOPE OF THE COUNT-BRIGHTNESS RELATION The first evidence for evolution using optically selected quasars was the pronounced non-Euclidean slope to $\log N(m)$ for quasars in the magnitude interval $18.1 < B < 21.4$ (Sandage & Luyten 1969). The three $N(m)$, B mag data points of (0.4, 18.1), (5, 19.4), and (100, 21.4) set out by these authors give $d \log N(m)/dm = 0.75$. This is much steeper than 0.6 for nonexpanding Euclidean space. The redshift K correction to the observed magnitude is close to zero, appropriate for a mean quasar spectrum of ν^{-1} (Sandage 1966). The observed slope is steeper than the $N(m)$ relation appropriate to expanding spaces, where $d \log N(m)/dm \sim 0.4$ is predicted from Figure 2.

Modern quasar counts, summarized by (among others) Mitchell et al. (1984) at the bright end and by Koo et al (1986, their Figure 7), Koo & Kron (1988b), and Boyle et al. (1987, their Figure 1) at the faint end, confirm these early numbers.

From the count data alone one cannot decide if the evolution is due to luminosity brightening with look-back time or to increased number of

objects (density evolution). Entrance to the large literature on this problem can be achieved from Schmidt & Green (1983) and from the review by Boyle et al. (1987). The 1987 consensus opinion is that the steep quasar count-magnitude distribution is due mainly to luminosity evolution.

7.4.2 DECREASE OF $dN(z)/dz$ AT HIGH z The possibility of a redshift cutoff at high z (≥ 3) was identified early in the analysis of radio quasars listed in the 3C Cambridge catalog. Observational selection effects in this *radio-selected* sample were assessed (Sandage 1972c), and none were found that could artificially produce the apparent cutoff, whose cause could be the first light from galaxies at high look-back times, i.e. from galaxy creation itself.

In the ensuing years, the reality of the quasar cutoff has been widely debated, usually by analyzing optically selected samples that have multiple selection effects not present in the radio samples. A number of deep surveys were begun early in quest of a cutoff. A review by Smith (1978) of the first phases of this activity sets the stage for Osmer's (1982) convincing study using optically selected quasars, where he concludes that "the apparent space density must decrease significantly at $3.7 < z < 4.7$."

In an independent deep survey using CCD detection with the Hale 200-inch reflector, Schmidt et al. (1986) concur. Their conclusion is that "quasars with an absolute magnitude of $M_B \sim -25$ suffer a redshift cutoff near or below a redshift of 3." A contrary discussion is given by Koo & Kron (1988b), who find no evidence for a redshift cutoff.

Any such large variation (if real) of any property of any type of object at large redshift is, of course, evidence for secular evolution of mean parameter values with look-back time. Convincing proof would be evidence for an evolving rather than a steady-state universe. If indeed evolution does occur, it is a most powerful, albeit elementary, verification of the most important prediction of the standard model—that the present Universe is of finite age. However, if secular evolution cannot be found where it should occur, the standard model fails. Although there are strong arguments in favor of evolution [Butcher-Oemler, Dressler-Gunn, quasar $N(m)$ slope, perhaps a redshift cutoff for quasars], the data in 1987 are not yet quite overwhelming.

8. ANGULAR DIAMETER OF RIGID RODS

8.1 *The Standard Model*

The theory of the angular diameter of a rigid rod at different distances in an expanding manifold was first worked out by Tolman (1930); it was discussed at greater length in his textbook (Tolman 1934) and also by

Hubble & Tolman (1935) and was put into modern notation by Sandage (1972a), who emphasized the difference between galaxy *metric* and *isophotal* diameters.

Let rR_1 be the coordinate interval between the observer and a galaxy at *light emission*. Because light rays travel along null geodesics in the expanding manifold, the angle θ between the rays from the extremities of the source is constant along the light path (neglecting the very small gravitational scattering due to intervening matter; cf. Gunn 1967, Kantowski 1969). Hence, upon reception, the angular size of a source of intrinsic size y (which does *not* expand with the manifold) is

$$\theta = \frac{y}{R_1 r}, \quad 43.$$

or, because $R_0 = R_1(1+z)$,

$$\theta = \frac{y(1+z)}{R_0 r}, \quad 44.$$

where $R_0 r$ is the coordinate interval of the source at the time of light reception given by Equation 30. Hence

$$\theta(\text{metric}) = \left(\frac{yH_0}{c} \right) \frac{q_0^2(1+z)^2}{q_0 z + (q_0 - 1)[-1 + (1 + 2q_0 z)^{1/2}]}. \quad 45.$$

Consider again the two instructive cases of $q_0 = 1/2$ and $q_0 = 0$, whose $R_0 r$ values are given by Equations 22 and 26, respectively. Hence, for $q_0 = 1/2$,

$$\theta\left(q_0 = \frac{1}{2}\right) = \left(\frac{yH_0}{2c} \right) \frac{(1+z)^{3/2}}{[\sqrt{1+z}-1]}, \quad 46.$$

and for $q_0 = 0$,

$$\theta(q_0 = 0) = \left(\frac{yH_0}{c} \right) \frac{(1+z)^2}{z\left(1 + \frac{z}{2}\right)}. \quad 47.$$

Galaxies do not have sharp edges; thus, measurements usually give isophotal diameters rather than metric. The two are not the same because in an expanding manifold, surface brightness is not constant with distance. The measured surface brightness is the received (apparent) flux divided by the apparent area, obtained by combining Equations 32 and 44, which gives

$$SB \sim \frac{f_b}{\theta^2} \sim (1+z)^{-4}, \quad 48.$$

independent of $R_0 r$. This means that Equation 48 is *model independent*, and therefore it does not depend on q_0 . This famous theorem was first proved by Tolman (1930). Note that if the manifold is not expanding, Equation 32 has but one $(1+z)$ factor, and, since $R_0 = R_1$,

$$SB(\text{nonexpanding}) \sim (1+z)^{-1}. \quad 49.$$

The difference between Equations 48 and 49 afford the well-known test (yet to be carried out properly) as to whether the manifold is truly expanding. Because isophotal diameters of galaxies differ from metric as a consequence of Equation 48, measurement of apparent diameters of galaxies to a given surface brightness *cannot* afford a test of Equation 48 (Sandage 1972a, Petrosian 1976, Tinsley 1976).

Suppose, in fact, that the manifold is *not* expanding and that the redshift is caused by some sort of energy decay of photons in the path to the observer. Although no mechanism has yet been proposed to avoid scattering of the photon beams in transit, and hence a blurring of distant images (not observed), nevertheless the predictions of this tired-light hypothesis are of interest.

Consider that the effect is linear with path length. Obviously then

$$1+z = \exp \frac{HRr}{c}, \quad 50.$$

from which

$$Rr = \frac{c}{H} \ln(1+z) \quad 51.$$

as a guess for flat space. In curved space the distance traveled is not Rr but rather $R \sin(HRr/c)$ for $k = +1$ and $R \sinh(HRr/c)$ for $k = -1$. Hence, in the case where the curvature factor is set to $HR/c = 1$ we have the possibilities

$$\theta = \frac{yH_0}{c} [\ln(1+z)]^{-1} \quad \text{for } k = 0, \quad 52.$$

$$\theta = \frac{yH_0}{c} \{\sin[\ln(1+z)]\}^{-1} \quad \text{for } k = +1, \quad 53.$$

$$\theta = \frac{yH_0}{c} \{\sinh[\ln(1+z)]\}^{-1} \quad \text{for } k = -1. \quad 54.$$

Return now to the expanding case of the standard model. It is instructive to expand Equation 45 in powers of z . The result is

$$\theta = \frac{yH_0}{c} [z^{-1} + 1/2(q_0 + 3) + O(z)] \quad 55.$$

for all q_0 . The leading term is z^{-1} , which can be shown also to be true for Equations 52–54. Hence both the standard model and the tired-light case require that angular metric diameters decrease as the inverse redshift for small z . This, of course, is the intuitive choice for a linear redshift–“distance” relation. [Note that in Segal’s (1975) speculation, $\theta \sim z^{-1/2}$ is the expectation]. The second-order term begins to be important for $z > 0.2$, causing the angular size to decrease more slowly than z^{-1} for all models. The predictions from the exact equations are shown in Figure 11, together with the intuitive $\theta \sim z^{-1}$ relation.

Hoyle (1959) was first to emphasize that for $q_0 > 0$, θ has a minimum at some finite z , larger than which the angular size increases. This is most easily seen by taking Equations 46 and 47 to their limits at large z . It is this that was believed to be the most direct geometrical test for the reality

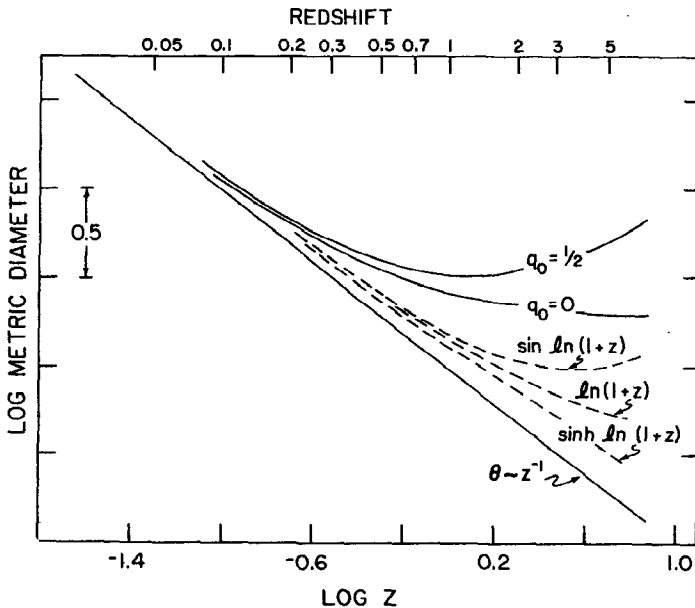


Figure 11 Theoretical angular size–redshift relations for $q_0 = 0$ and $q_0 = 1/2$ standard Friedmann models, and for three types of geometry for the tired-light speculation. The Euclidean $\theta \sim z^{-1}$ intuitive dependence is shown for purposes of comparison.

of expanding space. The effect has been sought in many observational tests (Section 8.3) but has not been found, raising what is the most serious doubt to date about the standard model because it questions whether the redshift is due to real expansion. Again, to save the phenomenon we must invoke evolution of the size of the standard rod in the look-back time. Before discussing the data at large look-back times, consider first the data at low redshift to test the leading term in the series expansions of Equations 45–47 and 52–54.

8.2 *Diameters of First-Ranked Cluster Galaxies at Low Redshift*

To test the z^{-1} dependence of Equation 45 at low redshift requires only a crude experiment. Furthermore, in this regime, isophotal and metric diameters are nearly the same. A photographic test made in 1970–71 using eye estimates of the angular diameters from Palomar Schmidt and 200-inch plates (Sandage 1972a) was sufficient to show that the dependence on z is z^{-1} , as in Equation 55. The data, set out in Figure 12, range in redshift from $z = 0.0023$ for the Leo group to $z = 0.46$ for 3C 295. Over this range, the isophotal diameters (to an isophote of ~ 23 mag arcsec $^{-2}$) range from ~ 250 arcsec to ~ 2 arcsec.

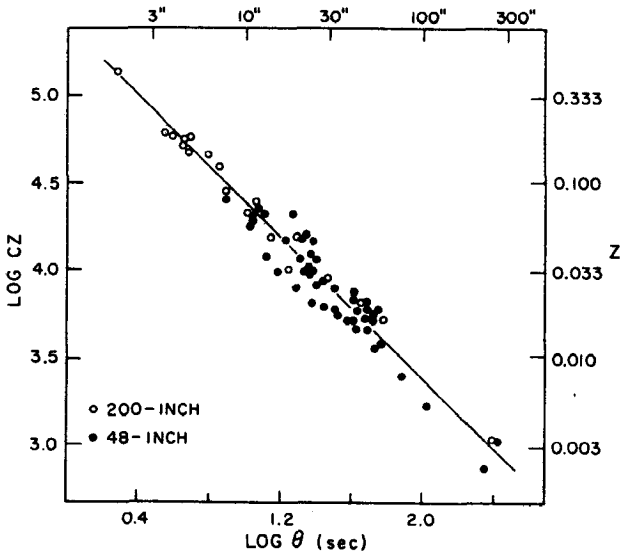


Figure 12 The observed $\theta(z)$ relation for low-redshift, first-ranked E cluster galaxies obtained by eye estimates from a homogeneous set of photographic plates. The line is the $\theta \sim z^{-1}$ Euclidean expectation (from Sandage 1972a).

This test of the linearity of the redshift-distance relation is independent of the $m(z)$ test of Section 4, although it is related to $m(z)$ under the assumption that all first-ranked E galaxies have only a small dispersion in surface brightness about a mean value. In the quoted paper, I called this premise the “constant” surface brightness condition, to which Gudehus (1975) pointed out the more proper statement now given—to wit, that a *stable* mean surface brightness with small dispersion exists that is independent of redshift at low redshift.

8.3 High-Redshift Data

8.3.1 RADIO SOURCES Hoyle’s (1959) prediction of a minimum in θ at a redshift of $z = 5/4$ for $q_0 = 1/2$ (and similar minima for other $q_0 > 0$) has been searched for extensively. Miley (1968, 1971) was among the first to apply the test to double-lobe radio sources, showing that they obey a z^{-1} relation over the entire redshift range that reaches $z = 2$. Selection effects were invoked to explain the lack of turnup of $\theta(z)$. Because the radio sources are from a catalog that is limited to a given (bright) radio flux level, there is a strong variation of *absolute* radio power with redshift (Sandage 1972c, his Figure 7). Hence, if the linear separation of the radio lobes varies with power, the observed z might be explained. Note that because $\theta(z)$ is smaller than expected at large redshift, such an explanation requires that the more powerful radio emitters have the smaller linear dimensions. (Those at largest z have the highest power due to the flux limitation of the source catalog.)

Following Miley (1968, 1971), the data discussed by Legg (1970), Wardle & Miley (1974), Swarup (1975), and Kapahi (1975, 1985) continued to show the same problem. Kapahi’s (1987, his Figure 7) comprehensive review of the most recent data again shows the need for size evolution of the sources, probably with look-back time rather than with radio power, to save the standard model.

8.3.2 CLUSTERS OF GALAXIES The variation with redshift of a characteristic angular size of clusters of galaxies has been sought. Various definitions of “size” have been proposed. The most complete study is that by Hickson (1977a,b), who used the harmonic mean separation of the brightest 40 galaxies within a specified radius from the center. The problem with this definition is that the specified radius of 3 Mpc depends on q_0 at large redshift. Bruzual & Spinrad (1978) show the partial degeneracy of this aperture-size problem to the galaxy selection with which to form the harmonic mean. Hickson (1977b; see also Hickson & Adams 1979) corrects for this effect by using the results of Monte Carlo simulations in the presence of field galaxies of given surface density, but the correction is

model dependent. Bruzual & Spinrad choose to analyze their independent data by fitting a theoretical density profile to galaxy counts so as to determine a core radius for each cluster, a method similar to that used by Bahcall [see Bahcall (1977) for a review].

In an analysis of both sets of data, Hickson & Adams (1979) conclude that "evolution in the linear cluster sizes is required for agreement with [the] models. Unless q_0 is considerably greater than 1, the mean cluster size is decreasing (i.e. evolving) at present with a time scale comparable to H_0^{-1} ." The combined data from the two studies, uncorrected for evolution, are shown in Figure 13 as set out by Hickson & Adams (1979, their Table 1). The data of Bruzual & Spinrad are closer to the Friedmann lines of $q_0 = 0$ and $q_0 = 1/2$ than those of Hickson & Adams (note the systematic difference of the two data sets at large redshift).

To first order, the z^{-1} dependence at small redshifts is again clearly evident in the data. However, for the second-order effect (i.e. the q_0 dependence) it is less certain that the data *can even be meaningful* because of the growing suspicion that clusters are not well-defined structures that have reached dynamic equilibrium. *Most clusters appear to be young aggregates*, still in the process of formation. The evidence comes from data on the Virgo cluster (Tully & Shaya 1984, Binggeli et al. 1987) and from the presence of substructure (multiple condensations) in most clusters studied in detail [Geller & Beers 1982, Baier 1983 (with many references to the earlier observational data), Beers & Tonry 1986]. Most important is the Dressler (1980) morphology-density effect *within a given cluster*, showing that virial mixing has *not* occurred.

With such pronounced subclustering, the meaning of the *core radius* or any other similar parameter becomes vague, depending on details of the *forming* cluster clumps. Measurement of the second-order curvature effect (i.e. q_0) using such an evolving metric rod must be questioned, despite its power to determine the gross first-order term.

8.3.3 METRIC DIAMETERS OF FIRST-RANKED CLUSTER GALAXIES It can be argued that the diameters of the brightest E *galaxies* in clusters are more stable than the sizes of the radio lobes of active galaxies or the sizes of clusters that are just forming. The evidence is the tightness of the $m(z)$ Hubble diagram (Figure 5) despite the question of cannibalism (Section 6.2.1), unless the cannibals operate with an effect that has an almost dispersionless progression with redshift. (In principle, cannibalism can be studied by finding different cannibal rates in clusters of different density.)

Metric diameters must be used in a test of Equation 48. Petrosian's (1976) definition of a metric diameter (his η index) has many advantages, such as its being nearly independent of luminosity evolution, of K correc-

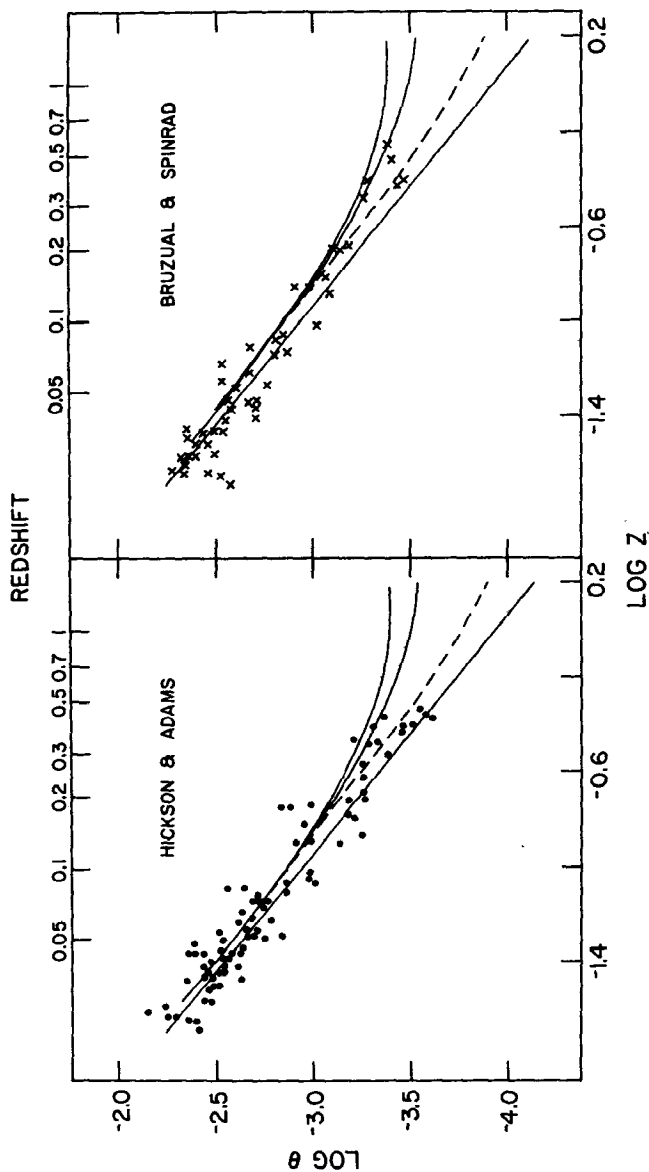


Figure 13 The observed $\theta(z)$ relations for cluster size determined by a harmonic mean algorithm (left) and by fitting a standard profile to obtain a cluster core radius (right). The theoretical curves from Figure 11 are superposed. Observational data are from Hickson & Adams (1979) and Bruzual & Spinrad (1978).

tion, and of the wavelength of observation. It is defined as the radius in the image at which the ratio of surface brightness, averaged over the area interior to that radius, to the SB at that radius is an adopted fixed number. Because it is a ratio, many corrections cancel.

Other examples of metric measures of size are the radius that contains half the light (called the “effective radius” in the literature); the Hubble a radius, where the SB falls to one fourth its “central” value; and the King core radius, where the SB is one half the “central” value. Central SB is never measured because of finite seeing disks, but a fitting parameter (I_0) can be inferred from global fits of the intermediate profile (i.e. for radii appropriately larger than the seeing disk).

A literature exists (cf. Oemler 1976, Kormendy 1977, Schombert 1986, Hoessel et al. 1987) on how some of these measures of radii vary with M_B of the parent galaxy and of the dispersion about the mean correlation, but no large study yet exists of the stability of the Petrosian η index for local galaxies. If it proves to be stable at some optimum SB ratio, the way would be open to test Equation 48 at large redshift. This is the only known test for the reality of the redshift, hence its extreme importance. The test has been tried by Geller & Peebles (1972), but it can be argued that they used isophotal rather than metric diameters, and further that they had only four data points.

Progress toward practical use of the Petrosian size has been reported by Djorgovski & Spinrad (1981). They measured the diameters of distant galaxies up to $z = 1.17$, but with only a few clusters to define the bright end. Their preliminary result is that the data, as measured, do not fit any part of the standard model parameter space (with $\Lambda = 0$), and that to do so again requires application of an evolutionary correction to the first-ranked galaxy sizes as a function of redshift. If the evolution is due to cannibalism, it can in principle be corrected by making the measurements on lower-ranked (fainter) cluster members that have not partaken of the cannibal’s feast.

The chief observational problem at the moment is that the angular diameter where $\eta = 2$ mag is ~ 2 arcsec at $z = 1$; this is subject then to seeing corrections from the ground in order to obtain a proper η value at this redshift.

9. TIME-SCALE TEST

9.1 *The Standard Model Prediction*

The value of the redshift-distance ratio (i.e. the Hubble constant) was first set at $H_0 = 558 \pm 10\% \text{ km s}^{-1} \text{ Mpc}^{-1}$ (Hubble & Humason 1931). Using this determination it was soon evident that the redshift of the galaxies is

a characteristic of the Universe itself, rather than being simply a local phenomenon. The evidence is the order-of-magnitude agreement between the expansion time scale associated with H_0^{-1} (which is 1.7×10^9 yr for $H_0 = 558$) and the age of the Earth, known even at the beginning of this century to be of order 10^9 yr [Holmes (1913), and many times thereafter following Boltwood (1907); cf. Holmes (1946, 1947, 1949) and Jeffreys (1924, 1948, 1949) for the early literature].

The conclusion was strengthened when the age of the oldest stars in the Galaxy was shown to be of the same order (Sandage & Schwarzschild 1952). This followed the earlier, several-decade debate on two time scales for the Galaxy. Bok (1946) reviewed the multiple evidence for the long and short time scale. Note from his review that even in 1946, evolution of stars was considered to be *up* rather than *off* the main sequence, giving no characteristic signal in the HR diagram by which to date the stars. This difficulty prevailed until Trumpler's (1925, 1928) discovery of main sequence termination points was theoretically understood in the early 1950s with the introduction of chemically inhomogeneous stellar models.

A third time scale was proposed by Rutherford (1929) that permitted age dating of the chemical elements. Ages of several times 10^9 yr for uranium was close enough to the Hubble time to be startling. In modern times the theme has been integrated into a general history of events that have spread the elements made in stars everywhere that there is matter (Hoyle 1946, 1947, 1954, Burbidge et al. 1957), setting the foundations for the study of the chemical evolution of galaxies.

Although order-of-magnitude agreement of the three cosmic clocks draws attention to the significance of the time-scale coincidence, a more detailed inquiry requires precision in the measurements. The standard model predicts the relation between the age of the Universe T_0 , the Hubble constant H_0 , and cosmological parameters q_0 (or Ω_0) and Λ . Many representations of this parameter space exist, such as that of Robertson (1955, 1963) for a specific value of H_0 ; of Fowler (1987), who generalized Robertson's parametrization by using Ω_0 and $H_0 T_0$ as axes; or of Stabell & Refsdal (1966, their Figure 5) in the density, q_0 plane with $H_0 T_0$ as parameter.

Figure 14 (from Sandage & Tammann 1986) is a diagram in the $H_0 T_0, \Lambda$ plane with Ω_0 as parameter, plotted from the tables of Refsdal et al. (1967) following Mattig (1958) and Solheim (1966). The well-known condition that $T_0 = 2/3 H_0^{-1}$ if $\Omega_0 = 1$ and $\Lambda = 0$ is marked by a crossed circle. Two other data points are marked by filled circles at values of H_0 and T_0 thought, in various past discussions, to be appropriate. The point to note about Figure 14 is that $H_0 T_0$, which is in principle observable, permits Ω_0 to be determined if Λ is known (or assumed); conversely, it permits Λ to

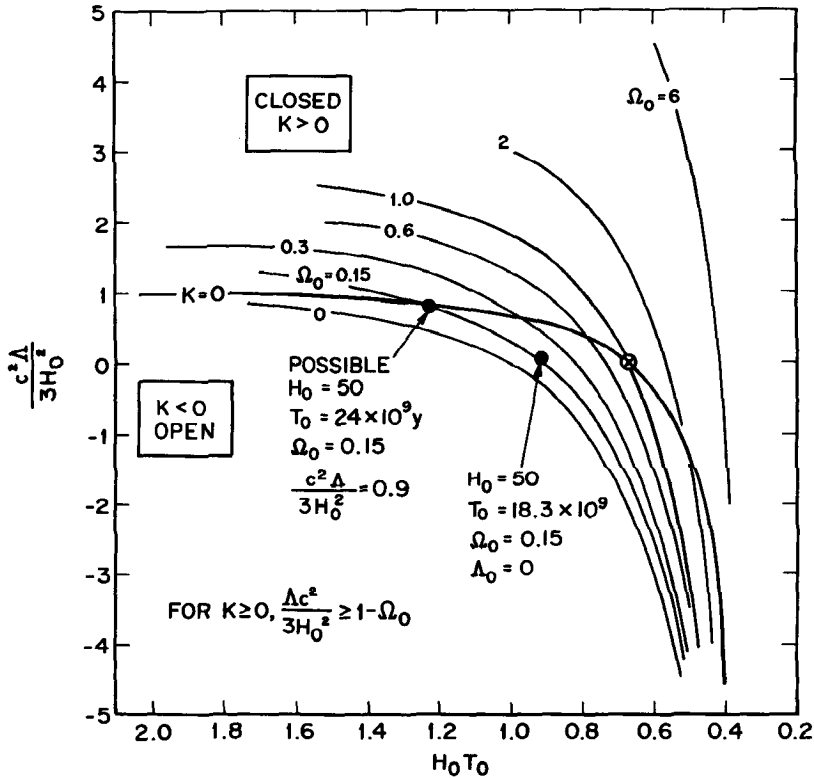


Figure 14 The time-scale test displayed in the H_0T_0, Λ plane with Ω_0 as parameter. The flat space-time condition of $\Lambda c^2 = 3H_0^2(1 - \Omega_0)$ is shown by the heavy line marked $K = 0$. The special case of $\Omega_0 = 1, \Lambda = 0, H_0T_0 = 2/3$ is marked by a crossed circle (from Sandage & Tammann 1986).

be found if H_0T_0 and Ω_0 are known. The special cut at $\Lambda = 0$ in the diagram gives the $\Omega_0 = f(H_0T_0)$ relation calculated earlier (Sandage 1961a, Table 8).

9.2 The Value of T_0 From the Chemical Elements and From the Oldest Stars

To use Figure 14 requires a knowledge of H_0 and the age of the Universe, found independently of the expansion data. The two methods to measure T_0 are (a) use of the age of the oldest stars in the Galaxy (to which the gestation time of galaxies is added), and (b) a determination of the age of the chemical elements. Entrance to the large literature on the second

problem is available in Burbidge et al. (1957), Dicke (1969), Cameron (1982), Fowler (1984), Thielemann & Truran (1986), Butcher (1987), Clayton (1987), and Cowan et al. (1987). The range in age in these references is wide, between $\sim 9 \times 10^9$ and $\sim 25 \times 10^9$ yr depending on assumptions such as sudden synthesis or gradual enrichment. Stronger statements on narrower limits enhance the literature, but no one has denied that the problem is model dependent in a way that is difficult to check. A forceful review that favors the short end of this range can be enjoyed from Fowler (1987).

The astronomical age dating of the Galaxy comes from measured globular cluster main sequence termination points, combined with stellar evolutionary model calculations for various helium and metal chemical compositions. Age estimates became stabilized in the early 1980s near 17×10^9 yr, based on generally accepted values of the chemical composition, the absolute magnitude M_v of the horizontal branches to set the termination luminosity, and models calculated by three principal groups (cf. Iben & Rood 1970, Ciardullo & Demarque 1977, Vandenberg 1983). The mean age of ~ 17 Gyr from the Yale (or Vandenberg) isochrones was based on distance moduli that use $M_v = 0.63$ mag for RR Lyrae stars of Osterhoff group II globular clusters and $M_v = 0.80$ mag for those of group I (Sandage 1982).

In a new development, observational evidence is becoming persuasive that the O/Fe chemical abundance ratio does not track with the Fe/H ratio in field subdwarfs of various Fe/H metallicities. An extensive review of the evidence is found in the ESO 1985 *Workshop on Production and Distribution of C,N,O Elements*, edited by Danziger et al. (1985). Following Simoda & Iben (1970), recent analyses by Vandenberg (1987), P. Demarque (private communication, 1987), and Rood & Crocker (1985) have independently shown that if the oxygen abundance remains high as the Fe/H ratio decreases, the age for a given turnoff luminosity *decreases* in the same way it would have decreased if Fe/H were increased. Vandenberg (1987) estimates that ages of globular clusters must be decreased by $\sim 15\%$ from the earlier values due to this effect of enhanced oxygen abundance in otherwise metal-poor stars if the effect in field subdwarfs occurs in globular cluster main sequence stars (but see Pilachowski 1988).

From this evidence and from a precision measurement of the age of 47 Tuc (Hesser et al. 1987), and adding 1.4 Gyr for the gestation time of the Galaxy, Sandage (1988a) adopted

$$T_0 = 14.9 \pm 2 \text{ Gyr}$$

for the age of the Universe from the age dating of stars.

9.3 Value of H_0

In these pages Hodge (1981) reviewed the debate up to ~ 1980 on the value of the Hubble constant, giving extensive references. Since that time attempts have been made to discover the source of the factor of 2 difference in H_0 between the long- and the short-distance scale workers. A factor of 2 in distance at a given redshift is equivalent to 1.5 magnitude (factor of 4 in luminosity). The source of the discrepancy must be sought and convincingly found if the matter is to be put to rest while members of the present generation are still active.

The factor of 2 is *not* in the local calibrators (Tammann 1987a,b), where at most only ~ 0.3 mag separates the various adopted calibrations. The explanation is almost certainly to be found as bias effects in the analysis of data from flux-limited catalogs, no matter what distance indicator is adopted, if that indicator is anything other than redshift. The proof of this statement is the *apparent increase of H_0 with redshift*, ranging from $50 \text{ km s}^{-1} \text{ Mpc}^{-1}$ locally to > 100 at ~ 4 times the Virgo cluster, obtained in all of the analyses by the advocates of the short scale (cf. de Vaucouleurs & Peters 1986, their Figure 2; Giraud 1986a,b, 1987). Discussions of this bias and why the apparent increase of H_0 with distance is an artifact include those by Teerikorpi (1975a,b, 1984, 1987), Sandage et al. (1979), Bottinelli et al. (see their 1987 and 1988 papers for a review), Kraan-Korteweg et al. (1986, 1988), and Sandage (1988a,b).

There have been many ways to discuss this type of Malmquist bias in flux-limited samples, most of which are complicated enough to be but dimly understood except, perhaps, by their authors. Figure 15 illustrates still another discussion of the effect and its consequences. Shown is a schematic $m(z)$ Hubble diagram using objects that have a spread in absolute magnitude M . Parallel envelope lines drawn to encompass the sample define the loci of absolute magnitudes M_1 and M_2 . (For a linear velocity-distance relation, recall that the slope of these lines is $dm/d\log z = 5$.) Divide the data into redshift zones, labeled 1–10 and shown hatched in Figure 15. If the sample is taken from a magnitude-limited catalog, there will be a limit line as shown, for which no objects in the sample are fainter. Consider now the mean (ridge) line of the data sample in the z, m plane. The true mean $\langle M_T \rangle$ value is seen in the data up to distance interval 4–5, but beyond that the data begin to be systematically too bright compared with the *true* value of $\langle M_T \rangle$.

What are the consequences? Suppose we assign an absolute magnitude $\langle M_T \rangle$ to each galaxy in the sample. For those closer than distance interval 5–6 we will make as many positive as negative errors in the correct $m - M$ distance modulus due to the luminosity spread in M . This part of the

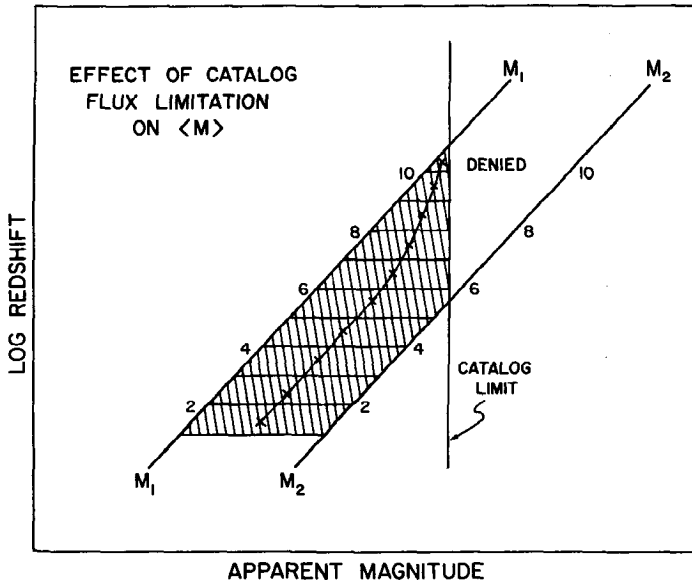


Figure 15 Illustration of the Malmquist bias as it affects the $m(z)$ Hubble diagram. Upper- and lower-envelope lines are shown that enclose the sample. The absolute magnitude M_1 is brighter than M_2 . The mean absolute magnitudes of the subsamples (crosses indicated at each distance interval) become progressively brighter with distance than the $\langle M \rangle$ value that applies to a complete (volume-limited) sample, valid for the data closer than distance limit number 5.

sample is distance limited. However, the flux limitation of the fainter sample progressively removes fainter absolute magnitudes from the remaining set as the true distance increases, giving false (biased) mean $m-M$ values. The inferred distances are too small in the mean for this subsample (because the $\langle M_T \rangle$ used is too faint to apply to it, as shown by the position of the crosses). By using these incorrect inferred photometric distances to obtain H_0 , progressively larger (incorrect) values of H_0 would be obtained as an artifact. Note that the correct value of H_0 is that obtained only in the distance interval closer than 5-6.

Detailed analysis of actual data (Sandage 1988a,b) has shown this bias explicitly in samples of ScI galaxies and in galaxies used for the Tully-Fisher distance scale method. By reading the data in the redshift limit of $z \rightarrow 0$, low values of H_0 have been obtained using the local calibrators with Cepheid distances. This is equivalent to the method of Richter & Huchtmeier (1984), who restrict their sample to the distance-limited list of Kraan-Korteweg & Tammann (1979) and obtain a low value of H_0 directly (cf. Sandage 1988b).

From these studies, together with a cluster data analysis with the Tully-Fisher method (Kraan-Korteweg et al. 1988), the value of the Hubble constant has been found to be in the range

$$42 \leq H_0 \leq 57 \text{ km s}^{-1} \text{ Mpc}^{-1},$$

where the formal error is adopted to be $\sim \pm 10\%$ from individual studies. The value found from supernovae of type Ia, using both an empirical (Sandage & Tammann 1982) and a theoretical calibration (Sutherland & Wheeler 1984, Arnett et al. 1985) of the absolute magnitude, gives (Cadonau et al. 1985)

$$H_0 = 43 \pm 10 \text{ km s}^{-1} \text{ Mpc}^{-1}, \quad 56.$$

which in turn gives a Hubble time of $H_0^{-1} = 22.7 \pm 5.5 \text{ Gyr}$.

9.4 *The Time Test of the Standard Model*

Of the four tests discussed earlier [$N(z)$, $N(m)$, $m(z)$, $\theta(z)$], the time test for q_0 is the only experiment devoid of direct evolutionary effects, making it the most promising (at the moment) to find q_0 (or Ω_0 if $\Lambda = 0$). Adopting $H_0 = 42 \pm 11 \text{ km s}^{-1} \text{ Mpc}^{-1}$ and $T_0 = 14.9 \pm 2 \text{ Gyr}$ (Sandage 1988a) gives

$$T_0 H_0 = 0.64 \pm 0.19,$$

which is close to the required $2/3$ if $\Omega_0 = +1$. The formal solution is

$$\Omega_0 = 1.2_{-0.9}^{+3.0}, \quad 57.$$

where the formal errors depend mostly on the large assigned error to H_0 . If we assign a smaller error and adopt $H_0 = 42 \pm 6$, then

$$\Omega_0 = 1.2_{-0.7}^{+1.6}.$$

Although the errors are still very large, there is now, for the first time, the astronomical possibility that $\Omega_0 = 1$ exactly, required by the inflationary cosmology of Grand Unification. It must be emphasized, however, that no claim is made here from the available data that Ω_0 is 1, only that it is now possible that it could be so if H_0 can be reduced, as here, to 42 and T_0 shortened by $\sim 15\%$ below 17 Gyr. This does give agreement with the inflationary prediction from the time-scale test, whereas the earlier literature values on ages did not.

Equation 31 shows that the price to be paid is to believe that at least 99% of the matter in the Universe is dark. Such dark matter has not yet been detected, and its existence must remain an article of faith for the true believer in the standard model and its covering theory of Grand Unification.

ACKNOWLEDGMENTS

This review is partially based on class notes from a lecture series on cosmology given at The Johns Hopkins University in the spring of 1987. It is a pleasure to thank the Department of Physics and Astronomy at JHU for the opportunity to lecture and to organize this work. Janet Krupsaw of JHU prepared an early version of part of the manuscript with her usual enthusiasm and skill. It is also a pleasure to thank Susan Drescher of the Mount Wilson and Las Campanas Observatories for her cheerful and careful preparation of so many drafts of the final manuscript. Special thanks are due David Layzer, who carefully read an early draft and made a number of suggestions to modify parts of the philosophical framework, and who also corrected misstatements of principle. Not all of his suggestions were taken, and remaining errors are claimed here by their owner. It is again a pleasure to acknowledge and to thank Keith Dodson of Annual Reviews for his careful, sensitive, and excellent job of textual editing.

Literature Cited

- Abell, G. 1958. *Ap. J. Suppl.* 3: 211
Alpher, R. A. 1948. *Phys. Rev.* 74: 1577
Alpher, R. A., Bethe, H. A., Gamow, G. 1948. *Phys. Rev.* 73: 803
Alpher, R. A., Folin, J. W., Herman, R. C. 1953. *Phys. Rev.* 92: 1347
Alpher, R. A., Herman, R. C. 1948. *Phys. Rev.* 74: 1737
Alpher, R. A., Herman, R. C. 1950. *Rev. Mod. Phys.* 22: 153
Arimoto, N., Yoshii, Y. 1986. *Astron. Astrophys.* 164: 260
Arimoto, N., Yoshii, Y. 1987. *Astron. Astrophys.* 173: 23
Arnett, W. D., Branch, D., Wheeler, J. C. 1985. *Nature* 314: 337
Backer, D. C., Hellings, R. W. 1986. *Ann. Rev. Astron. Astrophys.* 24: 537
Bahcall, N. 1977. *Ann. Rev. Astron. Astrophys.* 15: 505
Baier, F. W. 1983. *Astron. Nachr.* 304: 211
Balian, R., Audouze, J., Schramm, D. N., eds. 1979. *Physical Cosmology. Les Houches Summer Sch. No. 22.* Amsterdam: North-Holland
Bautz, L. P., Morgan, W. W. 1970. *Ap. J. Lett.* 162: L149
Beers, T. C., Tonry, J. L. 1986. *Ap. J.* 300: 557
Binggeli, B. 1987. In *Nearly Normal Galaxies*, ed. S. Faber, p. 195. New York: Springer-Verlag
Binggeli, B., Sandage, A., Tammann, G. A. 1988. *Ann. Rev. Astron. Astrophys.* 26: 509
Binggeli, B., Tammann, G. A., Sandage, A. 1987. *Astron. J.* 94: 251
Boesgaard, A. M., Steigman, G. 1985. *Ann. Rev. Astron. Astrophys.* 23: 319
Bok, B. J. 1931. *Harvard Circ. No. 371*
Bok, B. J. 1934. *Harvard Bull. No. 895*
Bok, B. J. 1937. *Distribution of Stars in Space*, p. 26-37. Chicago: Univ. Chicago Press
Bok, B. J. 1946. *MNRAS* 106: 61
Boltwood, B. B. 1907. *Am. J. Sci.* 23: 77
Bottinelli, L., Fougue, P., Gouguenheim, L., Paturel, G., Teerikorpi, P. 1987. *Astron. Astrophys.* 181: 1
Bottinelli, L., Gouguenheim, L., Paturel, G., Teerikorpi, P. 1986. *Astron. Astrophys.* 156: 157
Bottinelli, L., Gouguenheim, L., Paturel, G., Teerikorpi, P. 1988. *Ap. J.* 328: 4
Boyle, B. J., Shanks, T., Fong, R., Peterson, B. A. 1987. In *Observational Cosmology, IAU Symp. No. 124*, ed. A. Hewitt, G. Burbidge, L.-Z. Fang, p. 643. Dordrecht: Reidel
Broadhurst, T. J., Ellis, R. S., Shanks, T. 1987. *MNRAS*. In press
Brown, G. S., Tinsley, B. M. 1974. *Ap. J.* 194: 555
Bruck, H. A., Coyne, G. V., Longair, M.

- S., eds. 1982. *Astrophysical Cosmology*. Pontif. Acad. Sci. Scr. Varia. No. 48
- Bruzual, A. G. 1981. *Rev. Mex. Astron. Astrofis.* 6: 19
- Bruzual, A. G. 1983a. *Ap. J.* 273: 105
- Bruzual, A. G. 1983b. *Rev. Mex. Astron. Astrofis.* 8: 63
- Bruzual, A. G., Kron, R. G. 1980. *Ap. J.* 241: 25
- Bruzual, A. G., Spinrad, H. 1978. *Ap. J.* 220: 1
- Burbidge, E. M., Burbidge, G. R., Fowler, W. A., Hoyle, F. 1957. *Rev. Mod. Phys.* 29: 547
- Butcher, H. 1987. *Nature* 328: 127
- Butcher, H., Oemler, A. 1978a. *Ap. J.* 219: 18
- Butcher, H., Oemler, A. 1978b. *Ap. J.* 226: 559
- Butcher, H., Oemler, A. 1984a. *Ap. J.* 285: 426
- Butcher, H., Oemler, A. 1984b. *Nature* 310: 31
- Cadonau, R., Sandage, A., Tammann, G. A. 1985. In *Supernovae as Distance Indicators, Lect. Notes Phys.*, ed. N. Bartel, 224: 151. Berlin: Springer-Verlag
- Cameron, A. G. W. 1982. In *Essays in Nuclear Astrophysics*, ed. C. A. Barnes, D. D. Clayton, D. N. Schramm, p. 23. Cambridge: Cambridge Univ. Press
- Chincarini, G., Rood, H. J. 1976. *Ap. J.* 206: 30
- Ciardullo, R. 1986. PhD thesis. Yale Univ., New Haven, Conn.
- Ciardullo, R., Demarque, P. 1977. *Trans. Yale Univ. Obs.*, Vol. 33
- Clayton, D. D. 1987. *Nature* 329: 397
- Code, A. 1959. *Publ. Astron. Soc. Pac.* 71: 118
- Code, A. D., Welch, G. A. 1979. *Ap. J.* 228: 95
- Code, A. D., Welch, G. A., Page, T. L. 1972. In *The Scientific Results From the Orbiting Astronomical Observatory*, ed. A. D. Code, p. 559. Washington, DC: NASA
- Coleman, G. D., Wu, C. C., Weedman, D. W. 1980. *Ap. J. Suppl.* 43: 393
- Couch, W. J., Newell, E. B. 1984. *Ap. J. Suppl.* 56: 143
- Cowan, J. J., Thielemann, F.-K., Truran, J. W. 1987. *Ap. J.* 323: 543
- Crampin, J., Hoyle, F. 1961. *MNRAS* 122: 27
- Danziger, I. J., Matteucci, F., Kjær, K., eds. 1985. *ESO Workshop on Production and Distribution of C, N, O Elements*. Garching: ESO
- Davidson, W. 1959. *MNRAS* 119: 54
- DeGioia-Eastwood, K., Grasdalen, G. L. 1980. *Ap. J. Lett.* 239: L1
- de Lapparent, V., Geller, M., Huchra, J. 1986. *Ap. J. Lett.* 302: L1
- de Sitter, W. 1917. *MNRAS* 78: 3
- de Vaucouleurs, G. 1956. *Vistas Astron.* 2: 1584
- de Vaucouleurs, G. 1958. *Astron. J.* 63: 253
- de Vaucouleurs, G. 1960. *Ap. J. Suppl.* 5: 233
- de Vaucouleurs, G. 1970. *Science* 167: 1203
- de Vaucouleurs, G. 1972. In *External Galaxies and Quasistellar Objects, IAU Symp. No. 44*, ed. D. S. Evans, p. 353. Dordrecht: Reidel
- de Vaucouleurs, G., Malik, G. M. 1969. *MNRAS* 142: 387
- de Vaucouleurs, G., Peters, W. L. 1986. *Ap. J.* 303: 19
- de Vaucouleurs, G., de Vaucouleurs, A. 1972. *Mem. R. Astron. Soc.* 77: 1
- de Vaucouleurs, G., de Vaucouleurs, A., Corwin, H. G. 1977. *Second Reference Catalog of Bright Galaxies*. Austin: Univ. Tex. Press (RC2)
- Dicke, R. H. 1969. *Ap. J.* 155: 123
- Dicke, R. H., Peebles, P. J. E., Roll, P. G., Wilkinson, D. T. 1965. *Ap. J.* 142: 414
- Djorgovski, S., Spinrad, H. 1981. *Ap. J.* 251: 417
- Djorgovski, S., Spinrad, H. 1986. In preparation
- Djorgovski, S., Spinrad, H., Maar, J. 1985. In *New Aspects of Galaxy Photometry. Lect. Notes Phys.*, ed. J. L. Nieto, 232: 193. Berlin: Springer-Verlag
- Dressler, A. 1980. *Ap. J.* 236: 351
- Dressler, A. 1984. *Ann. Rev. Astron. Astrophys.* 22: 185
- Dressler, A., Faber, S. M., Burstein, D., Davies, R. L., Lynden-Bell, D. et al. 1987. *Ap. J. Lett.* 313: L37
- Dressler, A., Gunn, J. E. 1982. *Ap. J.* 263: 533
- Dressler, A., Gunn, J. E. 1983. *Ap. J.* 270: 7
- Dressler, A., Shectman, S. A. 1987. *Astron. J.* 94: 899
- Einstein, A. 1905. *Ann. Phys. (4)* 17: 891
- Ellis, G. F. R. 1984. *Ann. Rev. Astron. Astrophys.* 22: 157
- Ellis, R. S. 1983. In *The Origin and Evolution of Galaxies. NATO Adv. Study Inst.*, ed. B. J. T. Jones, J. E. Jones, p. 255. Dordrecht: Reidel
- Ellis, R. S. 1987. In *Observational Cosmology, IAU Symp. No. 124*, ed. A. Hewitt, G. Burbidge, L.-Z. Fang, p. 367. Dordrecht: Reidel
- Ellis, R. S. 1988. In *Towards Understanding Galaxies at Large Redshift*, ed. R. Kron, A. Renzini. Dordrecht: Reidel. In press
- Ellis, R. S., Couch, W. J., MacLaren, I., Koo, D. C. 1985. *MNRAS* 217: 239
- Ellis, R. S., Fong, R., Phillipps, S. 1977. *Nature* 265: 313
- Fath, E. A. 1914. *Astron. J.* 28: 75

- Field, G. B. 1972. *Ann. Rev. Astron. Astrophys.* 10: 227
- Fowler, W. A. 1984. *Rev. Mod. Phys.* 56: 149
- Fowler, W. A. 1987. *Q. J. R. Astron. Soc.* 28: 87
- Frogel, J. A., Persson, S. E., Aaronson, M., Matthews, K. 1978. *Ap. J.* 220: 75
- Gamow, G. 1946. *Phys. Rev.* 70: 572
- Gamow, G. 1948. *Phys. Rev.* 74: 505
- Geller, M. J., Beers, T. C. 1982. *Publ. Astron. Soc. Pac.* 94: 421
- Geller, M. J., Huchra, J. P. 1983. *Ap. J. Suppl.* 52: 61
- Geller, M. J., Peebles, P. J. E. 1972. *Ap. J.* 174: 1
- Geller, M. J., Peebles, P. J. E. 1976. *Ap. J.* 206: 939
- Geller, M. J., Postman, M. 1983. *Ap. J.* 274: 31
- Giraud, E. 1985. *Astron. Astrophys.* 153: 125
- Giraud, E. 1986a. *Ap. J.* 301: 7
- Giraud, E. 1986b. *Ap. J.* 309: 512
- Giraud, E. 1987. *Astron. Astrophys.* 174: 23
- Gott, J. R. 1977. *Ann. Rev. Astron. Astrophys.* 15: 235
- Gould, R. J. 1968. *Ann. Rev. Astron. Astrophys.* 6: 195
- Grasdalen, G. L. 1980. In *Objects of High Redshift, IAU Symp. No. 92*, ed. G. O. Abell, P. J. E. Peebles, p. 269. Dordrecht: Reidel
- Greenstein, J. L. 1938. *Ap. J.* 88: 605
- Gregory, S. A., Thompson, L. A. 1978. *Ap. J.* 222: 784
- Gudehus, D. H. 1975. *Publ. Astron. Soc. Pac.* 87: 763
- Gunn, J. E. 1967. *Ap. J.* 147: 61
- Gunn, J. E. 1978. In *The Friedmann Models and Optical Observations in Cosmology (Sas Fee Summer Sch.)*, ed. A. Maeder, L. Martinet, G. A. Tammann, p. 1. Saureverny: Geneva Obs.
- Gunn, J. E., Hoessel, J. G., Oke, J. B. 1986. *Ap. J.* 306: 30
- Gunn, J. E., Oke, J. B. 1975. *Ap. J.* 195: 255
- Hall, P., Mackay, C. D. 1984. *MNRAS* 210: 979
- Hamilton, D. 1985. *Ap. J.* 297: 371
- Hardcastle, J. A. 1914. *MNRAS* 74: 699
- Harrison, E. R. 1973. *Ann. Rev. Astron. Astrophys.* 11: 155
- Hausman, M. A., Ostriker, J. P. 1978. *Ap. J.* 224: 320
- Hawkins, G. 1962. *Nature* 194: 563
- Haynes, M. P., Giovanelli, R. 1986. *Ap. J. Lett.* 306: L55
- Heckman, T., Balick, B., Cranc, P. 1980. *Astron. Astrophys. Suppl.* 40: 295
- Heckmann, O. 1942. *Theorien der Kosmologie*. Berlin: Springer-Verlag
- Heiles, C. 1976. *Ap. J.* 204: 379
- Hesser, J. E., Harris, W. E., Vandenberg, D. A., Allwright, J. W. B., Shott, P., Stetson, P. 1987. *Publ. Astron. Soc. Pac.* 99: 739
- Hickson, P. 1977a. *Ap. J.* 217: 16
- Hickson, P. 1977b. *Ap. J.* 217: 964
- Hickson, P., Adams, P. J. 1979. *Ap. J. Lett.* 234: L91
- Hinks, A. R. 1911. *MNRAS* 71: 588
- Hodge, P. M. 1981. *Ann. Rev. Astron. Astrophys.* 19: 357
- Hoessel, J. G. 1980. *Ap. J.* 241: 493
- Hoessel, J. G., Gunn, J. E., Thuan, T. X. 1980. *Ap. J.* 241: 486
- Hoessel, J. G., Oegerle, W. R., Schneider, D. P. 1987. *Astron. J.* 94: 1111
- Holmberg, E. 1958. *Medd. Lund Obs., Ser. II, No. 136*
- Holmberg, E. 1974. *Astron. Astrophys.* 35: 121
- Holmes, A. 1913. *The Age of the Earth*. New York: Harper Brothers
- Holmes, A. 1946. *Nature* 157: 680
- Holmes, A. 1947. *Nature* 159: 127
- Holmes, A. 1949. *Nature* 163: 453
- Hoyle, F. 1946. *MNRAS* 106: 343
- Hoyle, F. 1947. *Proc. Phys. Soc. London* 59: 972
- Hoyle, F. 1954. *Ap. J. Suppl.* 1: 121
- Hoyle, F. 1959. In *Radio Astronomy, IAU Symp. No. 9*, ed. R. N. Bracewell, p. 529. Stanford, Calif: Stanford Univ. Press
- Hoyle, F., Sandage, A. 1956. *Publ. Astron. Soc. Pac.* 68: 301
- Hoyle, F., Wickramasinghe, N. C., Reddish, V. C. 1968. *Nature* 218: 1124
- Hubble, E. 1925a. *Observatory* 48: 139
- Hubble, E. 1925b. *Ap. J.* 62: 409
- Hubble, E. 1926. *Ap. J.* 64: 321
- Hubble, E. 1929. *Proc. Natl. Acad. Sci.* 15: 168
- Hubble, E. 1931. *Publ. Astron. Soc. Pac.* 43: 282
- Hubble, E. 1934. *Ap. J.* 79: 8
- Hubble, E. 1936a. *Ap. J.* 84: 270
- Hubble, E. 1936b. *Ap. J.* 84: 517
- Hubble, E. 1937. *The Observational Approach to Cosmology*. Oxford: Clarendon
- Hubble, E. 1953. *MNRAS* 113: 658
- Hubble, E., Humason, M. L. 1931. *Ap. J.* 74: 43
- Hubble, E., Tolman, R. C. 1935. *Ap. J.* 82: 302
- Huchra, J. P. 1977. *Ap. J.* 217: 928
- Huchra, J. P., Geller, M. J. 1982. *Ap. J.* 257: 423
- Humason, M. L. 1931. *Ap. J.* 74: 35
- Humason, M. L. 1936. *Ap. J.* 83: 10
- Humason, M. L., Mayall, N. U., Sandage, A. 1956. *Astron. J.* 61: 97 (HMS)
- Humboldt, A. V. 1866. *Cosmos*, 4: 25. New York: Harper Brothers
- Iben, I., Rood, R. T. 1970. *Ap. J.* 159: 605
- Jarvis, J. E., Tyson, J. A. 1981. *Astron. J.* 86: 476

- Jeffreys, H. 1924. *The Earth*, p. 61. Cambridge: Cambridge Univ. Press
- Jeffreys, H. 1948. *Nature* 162: 822
- Jeffreys, H. 1949. *Nature* 164: 1046
- Kantowski, R. 1969. *Ap. J.* 155: 89
- Kapahi, V. K. 1975. *MNRAS* 172: 513
- Kapahi, V. K. 1985. *MNRAS* 214: 19P
- Kapahi, V. K. 1987. In *Observational Cosmology, IAU Symp. No. 124*, ed. A. Hewitt, G. Burbidge, L.-Z. Fang, p. 251. Dordrecht: Reidel
- Kennedy, F. J., Thorndike, E. M. 1932. *Phys. Rev.* 42: 400
- Kimble, R., Davidsen, A., Sandage, A. 1987. *Bull. Am. Astron. Soc.* 19: 1062
- Kirshner, R. P., Oemler, A., Schechter, P. L. 1979. *Astron. J.* 84: 951
- Kirshner, R. P., Oemler, A., Schechter, P. L., Schectman, S. A. 1981. *Ap. J. Lett.* 248: L57
- Kolb, E. W., Turner, M. S., Lindley, D., Olive, K., Seckel, D., eds. 1986. *Inner Space/Outer Space*. Chicago: Univ. Chicago Press
- Koo, D. C. 1981. *Ap. J. Lett.* 251: L75
- Koo, D. C. 1988a. In *Towards Understanding Galaxies at Large Redshift*, ed. R. G. Kron, A. Renzini. Dordrecht: Reidel. In press
- Koo, D. C. 1988b. In *Evolution of Large Scale Structures in the Universe, IAU Symp. No. 130*, ed. J. Audouze, A. S. Szalay. Dordrecht: Reidel
- Koo, D. C., Kron, R. G. 1987. In *Observational Cosmology, IAU Symp. No. 124*, ed. A. Hewitt, G. Burbidge, L.-Z. Fang, p. 383. Dordrecht: Reidel
- Koo, D. C., Kron, R. G. 1988a. In *Towards Understanding Galaxies at Large Redshift*, ed. R. G. Kron, A. Renzini. Dordrecht: Reidel. In press
- Koo, D. C., Kron, R. C. 1988b. *Ap. J.* In press
- Koo, D. C., Kron, R. C., Cudworth, K. M. 1986. *Publ. Astron. Soc. Pac.* 98: 285
- Kormendy, J. 1977. *Ap. J.* 218: 333
- Kraan-Korteweg, R. C., Cameron, L. M., Tammann, G. A. 1986. In *Galaxy Distance and Deviations from Universal Expansion*, ed. B. F. Madore, R. B. Tully, p. 65. Dordrecht: Reidel
- Kraan-Korteweg, R. C., Cameron, L. M., Tammann, G. A. 1988. *Ap. J.* In press
- Kraan-Korteweg, R. C., Tammann, G. A. 1979. *Astron. Nachr.* 300: 181
- Kristian, J., Sandage, A., Westphal, J. 1978. *Ap. J.* 221: 383
- Kron, R. G. 1980a. *Ap. J. Suppl.* 43: 305
- Kron, R. G. 1980b. *Phys. Scr.* 21: 652
- Kron, R. G. 1982. *Vistas Astron.* 26: 37
- Kron, R. G., Renzini, A., eds. 1988. *Towards Understanding Galaxies at Large Redshift*. Dordrecht: Reidel. In press
- Larson, R. E., Tinsley, B. M. 1978. *Ap. J.* 219: 46
- Lasker, B. M. 1970. *Astron. J.* 75: 21
- LaViolette, P. 1986. *Ap. J.* 301: 544
- Layzer, D. 1987. Preprint
- Layzer, D., Hively, R. 1973. *Ap. J.* 179: 361
- Lebofsky, M. J. 1980. In *Objects of High Redshift, IAU Symp. No. 92*, ed. G. O. Abell, P. J. E. Peebles, p. 257. Dordrecht: Reidel
- Lebofsky, M. J. 1981. *Ap. J. Lett.* 245: L59
- Lebofsky, M. J., Eisenhardt, P. R. M. 1986. *Ap. J.* 300: 151
- Legg, T. H. 1970. *Nature* 226: 65
- Lilly, S. J. 1983. PhD thesis. Univ. Edinburgh, Scotland
- Lilly, S. J., Longair, M. S. 1982. *MNRAS* 199: 1053
- Lilly, S. J., Longair, M. S. 1984. *MNRAS* 211: 833
- Lilly, S. J., Longair, M. S., Allington-Smith, J. R. 1985. *MNRAS* 215: 37
- Loh, E. D. 1986. *Phys. Rev. Lett.* 57: 2865
- Loh, E. D., Spillar, E. J. 1986. *Ap. J. Lett.* 307: L1
- MacLaren, I., Ellis, R. S., Couch, W. J. 1988. *MNRAS* 230: 249
- Margenau, H. 1950. *The Nature of Physical Reality*. New York: McGraw-Hill
- Mathieu, R. D., Spinrad, H. 1981. *Ap. J.* 251: 485
- Mattig, W. 1958. *Astron. Nachr.* 284: 109
- Mattig, W. 1959. *Astron. Nachr.* 285: 1
- Mayall, N. U. 1934. *Lick Obs. Bull.* 16: 177 (No. 458)
- McClure, R. D., Crawford, D. L. 1971. *Astron. J.* 76: 31
- McVittie, G. C. 1956. *General Relativity and Cosmology*. London: Chapman & Hall. 1st ed.
- McVittie, G. C. 1965. *General Relativity and Cosmology*. London: Chapman & Hall. 2nd ed.
- McVittie, G. C. 1974. *Q. J. R. Astron. Soc.* 15: 246
- Mihalas, D., Binney, J. 1981. *Galactic Astronomy*, Chap. 4. San Francisco: Freeman
- Miley, G. 1968. *Nature* 218: 933
- Miley, G. K. 1971. *MNRAS* 152: 477
- Milne, E. A. 1935. *Relativity, Gravitation and World-Structure*. Oxford: Clarendon
- Misner, C. W., Thorne, K. S., Wheeler, J. A. 1973. *Gravitation*. San Francisco: Freeman
- Mitchell, K. J., Warnock, A., Usher, P. D. 1984. *Ap. J. Lett.* 287: L3
- Narlikar, J. V. 1983. *Introduction to Cosmology*. Boston: Jones & Bartlett
- Noonan, T. W. 1971. *Astron. J.* 76: 190
- Novikov, I. D., Zeldovich, Ya. B. 1967. *Ann. Rev. Astron. Astrophys.* 5: 627
- Oemler, A. 1976. *Ap. J.* 209: 693

- Oke, J. B. 1971. *Ap. J.* 170: 193
- Oke, J. B., Sandage, A. 1968. *Ap. J.* 154: 21
- Oort, J. H. 1983. *Ann. Rev. Astron. Astrophys.* 21: 373
- Osmer, P. S. 1982. *Ap. J.* 253: 28
- Osterbrock, D. E. 1984. *Ap. J. Lett.* 280: L43
- Ostriker, J. P., Hausman, M. A. 1977. *Ap. J. Lett.* 217: L125
- Ostriker, J. P., Tremaine, S. D. 1975. *Ap. J. Lett.* 202: L113
- Peach, J. V. 1969. *Nature* 223: 1140
- Peach, J. V. 1970. *Ap. J.* 159: 753
- Peach, J. V. 1972. In *External Galaxies and Quasistellar Objects*. IAU Symp. No. 44, ed. D. S. Evans, p. 314. Dordrecht: Reidel
- Pecker, J.-C., Vigier, J.-P. 1987. In *Observational Cosmology*. IAU Symp. No. 124, ed. A. Hewitt, G. Burbidge, L.-A. Fang, p. 507. Dordrecht: Reidel
- Peebles, P. J. E. 1966. *Ap. J.* 146: 542
- Peebles, P. J. E. 1968. *Ap. J.* 153: 13
- Peebles, P. J. E. 1969. *Nature* 224: 1093
- Peebles, P. J. E. 1971. *Physical Cosmology*. Princeton: Princeton Univ. Press
- Pence, W. 1976. *Ap. J.* 203: 39
- Penzias, A. A., Wilson, R. W. 1965. *Ap. J.* 142: 419
- Peterson, B. A. 1970a. *Ap. J.* 159: 333
- Peterson, B. A. 1970b. *Nature* 227: 54
- Peterson, B. A., Ellis, R. S., Kibblewhite, E. J., Bridgeland, M. T., Hooley, T., Horne, D. 1979. *Ap. J. Lett.* 233: L109
- Petrosian, V. 1976. *Ap. J. Lett.* 209: L1
- Pilachowski, C. A. 1988. *Ap. J. Lett.* 326: L57
- Proctor, R. A. 1869. *MNRAS* 29: 337
- Quirk, W. J., Tinsley, B. M. 1973. *Ap. J.* 170: 69
- Rana, N. C. 1981. *MNRAS* 197: 1125
- Refsdal, S., Stabell, R., deLange, F.-G. 1967. *Mem. R. Astron. Soc.* 71: 143
- Reichenbach, H. 1958. *The Philosophy of Space and Time*. New York: Dover
- Reynolds, J. H. 1920. *MNRAS* 81: 129, 598
- Reynolds, J. H. 1923a. *MNRAS* 83: 147
- Reynolds, J. H. 1923b. *MNRAS* 84: 76
- Richter, O.-G., Huchtmeier, W. K. 1984. *Astron. Astrophys.* 132: 253
- Rieke, M. 1984. Private communication (to Djorkovski & Spinrad)
- Robertson, H. P. 1929. *Proc. Natl. Acad. Sci. USA* 15: 822
- Robertson, H. P. 1933. *Rev. Mod. Phys.* 5: 62
- Robertson, H. P. 1935. *Ap. J.* 82: 284
- Robertson, H. P. 1938. *Z. Astrophys.* 15: 69
- Robertson, H. P. 1949. In *Albert Einstein: Philosopher-Scientist*, ed. P. A. Schilpp, p. 313. New York: Tudor
- Robertson, H. P. 1955. *Publ. Astron. Soc. Pac.* 67: 82
- Robertson, H. P. 1963. *Cosmology. Encyclopedia Britannica*. Vol. 6, p. 582
- Robertson, H. P., Noonan, T. 1968. *Relativity and Cosmology*, p. 359. Philadelphia: Saunders
- Roman, N. G. 1954. *Astron. J.* 59: 307
- Rood, R. T., Crocker, D. A. 1985. See Danziger et al. 1985, p. 61
- Rowan-Robinson, M. 1981. *Cosmology*. Oxford: Clarendon (2nd ed.)
- Rutherford, E. 1929. *Nature* 123: 313
- Sandage, A. 1953. In *Les Processus Nucléaires dans les Astres*, Liège Symp. Vol., p. 254. Louvain: Inst. Astrophys. Univ. Liège
- Sandage, A. 1957. *Ap. J.* 126: 326
- Sandage, A. 1958. *Vatican Conf. Stellar Populations. Specola Vaticana* 5: 41
- Sandage, A. 1961a. *Ap. J.* 133: 355
- Sandage, A. 1961b. *Ap. J.* 134: 916
- Sandage, A. 1963. *Ap. J.* 138: 863
- Sandage, A. 1966. *Ap. J.* 146: 13
- Sandage, A. 1972a. *Ap. J.* 173: 485
- Sandage, A. 1972b. *Ap. J.* 178: 1
- Sandage, A. 1972c. *Ap. J.* 178: 25
- Sandage, A. 1973a. *Ap. J.* 183: 711
- Sandage, A. 1973b. *Ap. J.* 183: 731
- Sandage, A. 1975a. *Ap. J.* 202: 563
- Sandage, A. 1975b. In *Galaxies and the Universe (Stars and Stellar Systems, Vol. 9)*, ed. A. Sandage, M. Sandage, J. Kristian, Chap. 19. Chicago: Univ. Chicago Press
- Sandage, A. 1976. *Ap. J.* 205: 6
- Sandage, A. 1978. *Astron. J.* 83: 904
- Sandage, A. 1982. *Ap. J.* 252: 553
- Sandage, A. 1986. *Ap. J.* 307: 1
- Sandage, A. 1988a. *Ap. J.* In press
- Sandage, A. 1988b. *Ap. J.* In press
- Sandage, A., Eggen, O. J. 1959. *MNRAS* 119: 278
- Sandage, A., Hardy, E. 1973. *Ap. J.* 183: 743
- Sandage, A., Kristian, J., Westphal, J. A. 1976. *Ap. J.* 205: 688
- Sandage, A., Luyten, W. J. 1969. *Ap. J.* 155: 913
- Sandage, A., Schwarzschild, M. 1952. *Ap. J.* 116: 463
- Sandage, A., Tammann, G. A. 1981. *A Revised Shapley-Ames Catalog of Bright Galaxies*. Carnegie Inst. Washington Publ. 635 (RSA)
- Sandage, A., Tammann, G. A. 1982. *Ap. J.* 256: 339
- Sandage, A., Tammann, G. A. 1986. See Kolb et al. 1986, p. 41
- Sandage, A., Tammann, G. A., Hardy, E. 1972. *Ap. J.* 172: 253
- Sandage, A., Tammann, G. A., Yahil, A. 1979. *Ap. J.* 232: 352
- Sandage, A., Visvanathan, N. 1978. *Ap. J.* 223: 707
- Schechter, P., Peebles, P. J. E. 1976. *Ap. J.* 209: 670
- Schild, R., Oke, J. B. 1971. *Ap. J.* 169: 209

- Schmidt, M., Green, R. F. 1983. *Ap. J.* 269: 352
- Schmidt, M., Schneider, D. P., Gunn, J. E. 1986. *Ap. J.* 306: 411
- Schneider, D. P., Gunn, J. E., Hoessel, J. G. 1983a. *Ap. J.* 264: 337
- Schneider, D. P., Gunn, J. E., Hoessel, J. G. 1983b. *Ap. J.* 268: 476
- Schombert, J. M. 1986. *Ap. J. Suppl.* 60: 603
- Seares, F. 1925. *Ap. J.* 62: 168
- Searle, L., Sargent, W. L. W., Bagnuolo, W. G. 1973. *Ap. J.* 179: 427
- Sebok, W. L. 1986. *Ap. J. Suppl.* 62: 301
- Segal, I. 1975. *Proc. Natl. Acad. Sci.* 72: 2473
- Segal, I. E. 1976. *Mathematical Cosmology and Extragalactic Astronomy*, p. 104. New York: Academic
- Segal, I. 1981. *Proc. Natl. Acad. Sci. USA* 77: 10
- Seldner, M., Siebers, B., Groth, E. J., Peebles, P. J. E. 1977. *Astron. J.* 82: 249
- Setti, G., Van Hove, L., eds. 1983. *Cosmology and Fundamental Physics. ESO/CERN Workshop, 1st*. Geneva: CERN
- Shane, C. D. 1975. In *Galaxies and the Universe (Stars and Stellar Systems, Vol. 9)*, ed. A. Sandage, M. Sandage, J. Kristian, Chap. 16. Chicago: Univ. Chicago Press
- Shane, C. D., Wirtanen, C. A. 1950. *Proc. Am. Philos. Soc.* 94: 13
- Shane, C. D., Wirtanen, C. A. 1954. *Astron. J.* 59: 285
- Shane, C. D., Wirtanen, C. A. 1967. *Publ. Lick Obs.* 22: 1
- Shanks, T., Stevenson, P. R. F., Fong, R., MacGillivray, H. T. 1984. *MNRAS* 206: 767
- Shapley, H. 1932. *Harv. Bull. No. 890*
- Shapley, H., Ames, A. 1932. *Harvard Ann.* 88. No. 2
- Simoda, M., Iben, I. 1970. *Ap. J. Suppl.* 22: 81
- Smith, M. G. 1978. *Vistas Astron.* 22: 321
- Solheim, J.-E. 1966. *MNRAS* 133: 321
- Spinrad, H. 1977. In *The Evolution of Galaxies and Stellar Populations*, ed. B. M. Tinsley, R. B. Larson, p. 301. New Haven, Conn: Yale Univ. Press
- Spinrad, H. 1980. In *Objects of High Redshift, IAU Symp. No. 92*, ed. G. O. Abell, P. J. E. Peebles, p. 39. Dordrecht: Reidel
- Spinrad, H. 1986. *Publ. Astron. Soc. Pac.* 98: 269
- Spinrad, H., Djorgovski, S. 1987. In *Observational Cosmology, IAU Symp. No. 124*, ed. A. Hewitt, G. Burbidge, L.-Z. Fang, p. 129. Dordrecht: Reidel
- Stabell, R., Refsdal, S. 1966. *MNRAS* 132: 379
- Stebbins, J., Whitford, A. E. 1948. *Ap. J.* 108: 413
- Steigman, G. 1976. *Ann. Rev. Astron. Astrophys.* 14: 339
- Strömberg, B. 1966. *Ann. Rev. Astron. Astrophys.* 4: 433
- Sunyaev, R. A., Zeldovich, Ya. B. 1980. *Ann. Rev. Astron. Astrophys.* 18: 537
- Sutherland, P. G., Wheeler, J. C. 1984. *Ap. J.* 280: 282
- Swarup, G. 1975. *MNRAS* 172: 501
- Tammann, G. A. 1987a. *Tex. Symp. Relativ. Astrophys., 13th*
- Tammann, G. A. 1987b. In *Observational Cosmology, IAU Symp. No. 124*, ed. A. Hewitt, G. Burbidge, L.-Z. Fang, p. 151. Dordrecht: Reidel
- Tammann, G. A., Sandage, A. 1985. *Ap. J.* 294: 81
- Tammann, G. A., Yahil, A., Sandage, A. 1979. *Ap. J.* 234: 775
- Teerikorpi, P. 1975a. *Astron. Astrophys.* 45: 117
- Teerikorpi, P. 1975b. *Observatory* 95: 105
- Teerikorpi, P. 1984. *Astron. Astrophys.* 141: 407
- Teerikorpi, P. 1987. *Astron. Astrophys.* 173: 39
- Thaddeus, P. 1972. *Ann. Rev. Astron. Astrophys.* 10: 305
- Thielemann, F.-K., Truran, J. W. 1986. In *Galaxy Distances and Deviations From Universal Expansion*, ed. B. F. Madore, R. B. Tully, p. 185. Dordrecht: Reidel
- Tift, W. G. 1963. *Astron. J.* 68: 302
- Tift, W. G. 1969. *Astron. J.* 74: 354
- Tift, W. G., Gregory, S. A. 1976. *Ap. J.* 205: 696
- Tinsley, B. M. 1968. *Ap. J.* 151: 547
- Tinsley, B. M. 1972a. *Ap. J. Lett.* 173: L93
- Tinsley, B. M. 1972b. *Astron. Astrophys.* 20: 383
- Tinsley, B. M. 1976. *Ap. J.* 203: 63
- Tinsley, B. M. 1977a. In *The Expansion of the Universe, IAU Colloq. No. 37*, ed. C. Balkowski, B. E. Westerlund, p. 223. Paris: CNRS
- Tinsley, B. M. 1977b. *Ap. J.* 211: 621
- Tinsley, B. M. 1978. *Ap. J.* 222: 14
- Tinsley, B. M. 1980. *Ap. J.* 241: 41
- Tinsley, B. M., Gunn, J. E. 1976. *Ap. J.* 203: 52
- Tolman, R. C. 1930. *Proc. Natl. Acad. Sci. USA* 16: 511
- Tolman, R. C. 1934. *Relativity, Thermodynamics, and Cosmology*, p. 467. Oxford: Clarendon
- Tremaine, S. D. 1981. In *The Structure and Evolution of Normal Galaxies*, ed. S. M. Fall, D. Lynden-Bell, p. 67. Cambridge: Univ. Cambridge Press
- Tremaine, S. D., Richstone, D. O. 1977. *Ap. J.* 212: 311
- Trumpler, R. J. 1925. *Publ. Astron. Soc. Pac.* 37: 307

- Trumpler, R. J. 1928. *Publ. Astron. Soc. Pac.* 40: 265
- Tully, R. B., Shaya, J. 1984. *Ap. J.* 281: 31
- VandenBerg, D. 1983. *Ap. J. Suppl.* 51: 29
- VandenBerg, D. 1987. In *Globular Cluster Systems Around Galaxies, IAU Symp. No. 126*, ed. J. Grindlay, A. G. D. Philip, p. 107. Dordrecht: Reidel
- von der Pahlen 1937. *Lehrbuch der Stellarstatistik No. 428*. Leipzig: Barth
- Wagoner, R. V. 1973. *Ap. J.* 179: 343
- Wagoner, R. V., Fowler, W. A., Hoyle, F. 1967. *Ap. J.* 148: 3
- Walker, A. G. 1936. *Proc. London Math. Soc. 2nd Ser.* 42: 90
- Wardle, J. F. C., Miley, G. K. 1974. *Astron. Astrophys.* 30: 305
- Weinberg, S. E. 1972. *Gravitation and Cosmology*. New York: Wiley
- Weiss, R. 1980. *Ann. Rev. Astron. Astrophys.* 18: 489
- Wells, D. C. 1972. *Univ. Tex. Publ. No. 13*
- Whitford, A. E. 1954. *Ap. J.* 120: 599
- Whitford, A. E. 1971. *Ap. J.* 169: 215
- Whittaker, E. T. 1958. *From Euclid to Eddington*. New York: Dover
- Wilkinson, A., Oke, J. B. 1978. *Ap. J.* 220: 376
- Will, C. M. 1981. *Theory and Experiment in Gravitational Physics*. Cambridge: Cambridge Univ. Press
- Wirth, A., Gallagher, J. S. 1980. *Ap. J.* 242: 469
- Wolfendale, A. W., ed. 1981. *Progress in Cosmology Symposium, Proceedings, Vol. 99*. Dordrecht: Reidel
- Yee, H. K. D., Green, R. F. 1987. *Ap. J.* 319: 28
- Yoshii, Y., Takahara, F. 1988. *Ap. J.* 326: 1
- Zeldovich, Ya. B. 1965. *Adv. Astron. Astrophys.* 3: 241
- Zeldovich, Ya. B., Novikov, I. D. 1983. *Relativistic Astrophysics, Vol. 2*. Chicago: Univ. Chicago Press
- Zwicky, F. 1957. *Morphological Astronomy*, p. 81. Berlin: Springer-Verlag



CONTENTS

A MORPHOLOGICAL LIFE, <i>W. W. Morgan</i>	1
A POSTENCOUNTER VIEW OF COMETS, <i>D. A. Mendis</i>	11
THE GALACTIC NUCLEAR BULGE AND THE STELLAR CONTENT OF SPHEROIDAL SYSTEMS, <i>Jay A. Frogel</i>	51
POLARIZATION PROPERTIES OF EXTRAGALACTIC RADIO SOURCES, <i>D. J. Saikia and C. J. Salter</i>	93
LARGE-SCALE EXPANDING SUPERSTRUCTURES IN GALAXIES, <i>Guillermo Tenorio-Tagle and Peter Bodenheimer</i>	145
TESTS OF EVOLUTIONARY SEQUENCES USING COLOR-MAGNITUDE DIAGRAMS OF GLOBULAR CLUSTERS, <i>Alvio Renzini and Flavio Fusi Pecci</i>	199
VOIDS, <i>H. J. Rood</i>	245
SUPERNOVAE AND SUPERNOVA REMNANTS, <i>Kurt W. Weiler and Richard A. Sramek</i>	295
ENHANCED STAR FORMATION AND INFRARED EMISSION IN THE CENTERS OF GALAXIES, <i>Charles M. Telesco</i>	343
THE INFRARED TEMPORAL DEVELOPMENT OF CLASSICAL NOVAE, <i>Robert D. Gehrz</i>	377
RECENT ADVANCES IN OPTICAL ASTROMETRY, <i>David G. Monet</i>	413
ORIGIN OF THE SOLAR SYSTEM, <i>A. G. W. Cameron</i>	441
OBSERVED VARIABILITY OF THE SOLAR LUMINOSITY, <i>H. S. Hudson</i>	473
THE LUMINOSITY FUNCTION OF GALAXIES, <i>Bruno Binggeli, Allan Sandage, and G. A. Tammann</i>	509
OBSERVATIONAL TESTS OF WORLD MODELS, <i>Allan Sandage</i>	561
LARGE-SCALE STRUCTURE IN THE UNIVERSE INDICATED BY GALAXY CLUSTERS, <i>Neta A. Bahcall</i>	631
INDEXES	
Subject Index	687
Cumulative Index of Contributing Authors, Volumes 16–26	696
Cumulative Index of Chapter Titles, Volumes 16–26	698